

Accepted Manuscript

Investigation of B,C-Ring Truncated Deguelin Derivatives as Heat Shock Protein 90 (HSP90) Inhibitors for Use as Anti-Breast Cancer Agents

Ho Shin Kim, Van-Hai Hoang, Mannkyu Hong, Kyung Chul Kim, Jihyae Ann, Cong-Truong Nguyen, Ji Hae Seo, Hoon Choi, Jun Yong Kim, Kyu-Won Kim, Woong Sub Byun, Sangkook Lee, Seungbeom Lee, Young-Ger Suh, Jie Chen, Hyun-Ju Park, Tae-Min Cho, Ji Young Kim, Jae Hong Seo, Jeewoo Lee

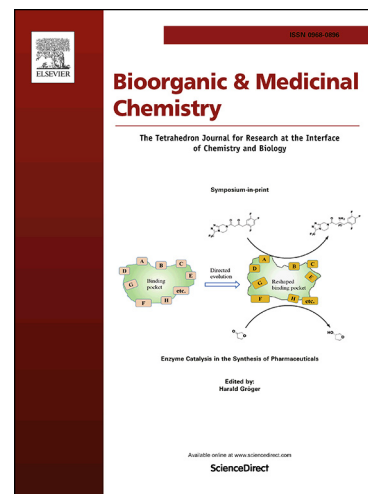
PII: S0968-0896(19)30117-8
DOI: <https://doi.org/10.1016/j.bmc.2019.02.040>
Reference: BMC 14776

To appear in: *Bioorganic & Medicinal Chemistry*

Received Date: 22 January 2019
Revised Date: 19 February 2019
Accepted Date: 19 February 2019

Please cite this article as: Kim, H.S., Hoang, V-H., Hong, M., Chul Kim, K., Ann, J., Nguyen, C-T., Seo, J.H., Choi, H., Yong Kim, J., Kim, K-W., Sub Byun, W., Lee, S., Lee, S., Suh, Y-G., Chen, J., Park, H-J., Cho, T-M., Kim, J.Y., Seo, J.H., Lee, J., Investigation of B,C-Ring Truncated Deguelin Derivatives as Heat Shock Protein 90 (HSP90) Inhibitors for Use as Anti-Breast Cancer Agents, *Bioorganic & Medicinal Chemistry* (2019), doi: <https://doi.org/10.1016/j.bmc.2019.02.040>

This is a PDF file of an unedited manuscript that has been accepted for publication. As a service to our customers we are providing this early version of the manuscript. The manuscript will undergo copyediting, typesetting, and review of the resulting proof before it is published in its final form. Please note that during the production process errors may be discovered which could affect the content, and all legal disclaimers that apply to the journal pertain.



Investigation of B,C-Ring Truncated Deguelin Derivatives as Heat Shock Protein 90 (HSP90) Inhibitors for Use as Anti-Breast Cancer Agents

Ho Shin Kim ^a, Van-Hai Hoang ^a, Mannkyu Hong ^a, Kyung Chul Kim ^a, Jihyae Ann ^a, Cong-Truong Nguyen ^a, Ji Hae Seo ^a, Hoon Choi ^a, Jun Yong Kim ^a, Kyu-Won Kim ^a, Woong Sub Byun ^a, Sangkook Lee ^a, Seungbeom Lee ^a, Young-Ger Suh ^{a,b}, Jie Chen ^c, Hyun-Ju Park ^c, Tae-Min Cho ^{d,e}, Ji Young Kim ^d, Jae Hong Seo ^{d,e,*}, Jeewoo Lee ^{a,*}

^a College of Pharmacy, Seoul National University, Seoul 08826, Korea

^b College of Pharmacy, CHA University, Gyeonggi-do 11160, Korea

^c School of Pharmacy, Sungkyunkwan University, Suwon, Gyeonggi-do 16419, South Korea

^d Division of Medical Oncology, Department of Internal Medicine, Korea University College of Medicine, Korea University, Seoul 152-703, Republic of Korea.

^e Brain Korea 21 Program for Biomedical Science, Korea University College of Medicine, Korea University, Seoul 152-703, Republic of Korea.

* Corresponding Authors

Jeewoo Lee, Ph.D.

Phone: 82-2-880-7846

Fax: 82-2-888-0649

E-mail: jeewoo@snu.ac.kr

Jae Hong Seo, Ph.D.

E-mail: cancer@korea.ac.kr

Key Words: Heat Shock Protein 90; HSP90; Hypoxia Inducible Factor-1 α ; HIF-1 α ; Antitumor; Breast Cancer; Deguelin

Abstract

On the basis of deguelin, a series of the B,C-ring truncated surrogates with *N*-substituted amide linkers were investigated as HSP90 inhibitors. The structure activity relationship of the template was studied by incorporating various substitutions on the nitrogen of the amide linker and examining their HIF-1 α inhibition. Among them, compound **57** showed potent HIF-1 α inhibition and cytotoxicity in triple-negative breast cancer lines in a dose-dependent manner. Compound **57** downregulated expression and phosphorylation of major client proteins of HSP90 including AKT, ERK and STAT3, indicating that its antitumor activity was derived from the inhibition of HSP90 function. The molecular modeling of **57** demonstrated that **57** bound well to the C-terminal ATP-binding pocket in the open conformation of the *h*HSP90 homodimer with hydrogen bonding and pi-cation interactions. Overall, compound **57** is a potential antitumor agent for triple-negative breast cancer as a HSP90 C-terminal inhibitor.

1. Introduction

Heat shock protein 90 (HSP90) is a molecular chaperone involved in the folding, maturation, and degradation of its client proteins, which are associated with hallmarks of cancer.¹⁻³ Thus, inhibition of HSP90 has attracted much attention as a new and effective cancer therapy, particularly to overcome resistance to anticancer agents.⁴⁻⁶ Structurally, HSP90 is a homodimeric protein of ~90 kDa in which each monomer contains an *N*-terminal ATP-binding domain, a middle cochaperone and client-binding domain, and a *C*-terminal dimerization domain. Most HSP90 inhibitors that have been developed have been identified as the *N*-term inhibitors that bind to an ATP-binding domain in the *N*-terminal.^{7,8} However, one of the main drawbacks in these inhibitors is the induction of a heat shock response (HSR), which ultimately leads to an increase in HSP90 and anti-apoptotic proteins such as HSP70 and HSP27. Therefore, the inhibition of another ATP-binding site in the *C*-terminal provides an alternative strategy to overcome these side effects.⁹⁻¹² Indeed, novobiocin, the first *C*-terminal inhibitor discovered, has shown potency in several cancer cell lines as it degrades clients without reported HSR.¹³ Hypoxia Inducible Factor-1 α (HIF-1 α) is a transcription factor, one of the HSP90 client proteins, that regulates the cellular response for the survival of cells in hypoxia. Because this regulation can induce angiogenesis, proliferation, metastasis and invasion of cancer cells,^{14,15} HIF-1 α inhibition through HSP90 modulation can inhibit the angiogenesis and proliferation of cancer cells and reduce chemotherapy resistance.^{16,17}

Triple-negative breast cancer (TNBC) is a highly heterogeneous and biologically aggressive cancer which is associated with a poor clinical outcome due to the lack of established molecular targets, such as estrogen receptor (ER), progesterone receptor (PR) and human epidermal growth factor receptor 2 (HER2).¹⁸ Elevated HSP90 levels are frequently found in TNBC patients and are significantly correlated with a higher risk of recurrence and distant metastasis, leading to poor prognoses.¹⁹ Emerging preclinical evidence highlights that HSP90 inhibition impairs cell proliferation, cell invasion, motility and angiogenesis as well as cell propagation in solid cancers via dysregulation of HSP90 client proteins, including EGFR, MEK, STAT, and AKT.²⁰⁻²³ Of particular

note, the growth of TNBC is tightly governed by the activation of these HSP90 clients²⁴⁻²⁶; thus, targeting HSP90 may provide an effective therapeutic strategy for the treatment of TNBC.

Deguelin (**1**), a naturally occurring rotenoid, showed potent antitumor activity by inhibiting ATP binding to the C-terminal of heat shock protein (HSP90), leading to the decomposition of HIF-1 α .²⁷ To discover a novel scaffold for a C-terminal HSP90 inhibitor based on deguelin, we have investigated simplified deguelin analogues through a ring-truncation approach. Among them, compounds **2** and **3**, designed as B,C-ring truncated templates, exhibited excellent HIF-1 α suppression and potent cell growth inhibition in a human nonsmall-cell lung carcinoma cell line (H1299) comparable to deguelin (**Figure 1**).²⁸ Mechanistic studies revealed that these compounds disrupted HSP90 function by binding to its C-terminal ATP-binding pocket and interfering with the interaction with its cochaperones and client proteins, triggering their degradation.²⁹

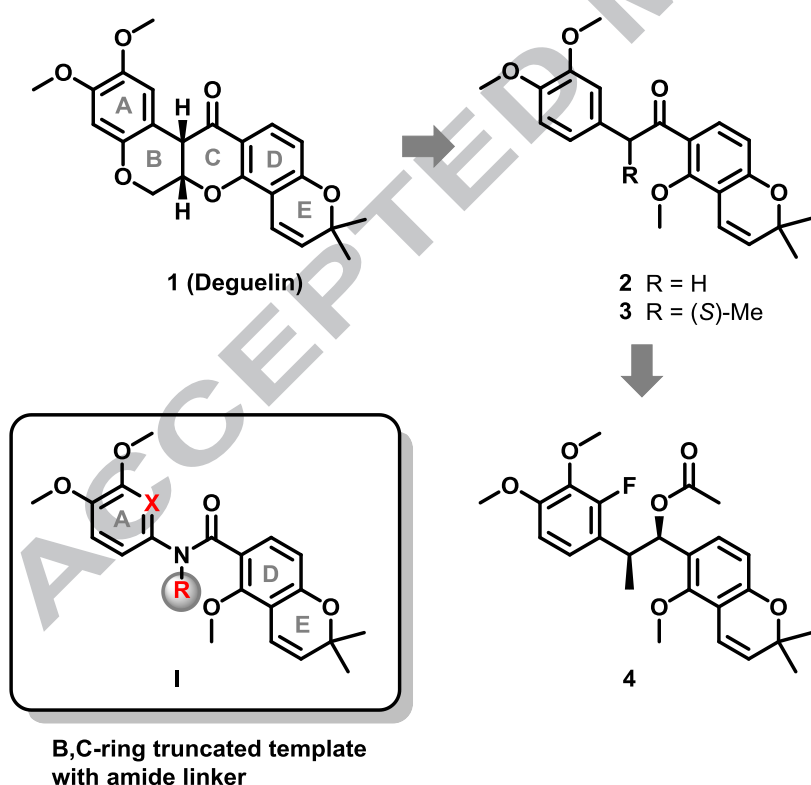


Figure 1. Deguelin and its B,C-ring-truncated surrogates

Recently, we reported a series of fluorophenyl and pyridine surrogates of **2** and **3** with modified linkers for HIF-1 α inhibition.³⁰ Among them, several compounds showed better HIF-1 α inhibition than deguelin, **2** and **3**. In particular, compound **4** exhibited promising anticancer and antiangiogenic activities. The docking study of **4** indicated that its cytotoxicity was derived from HIF-1 α destabilization by binding to the C-terminal ATP-binding site of HSP90.³⁰

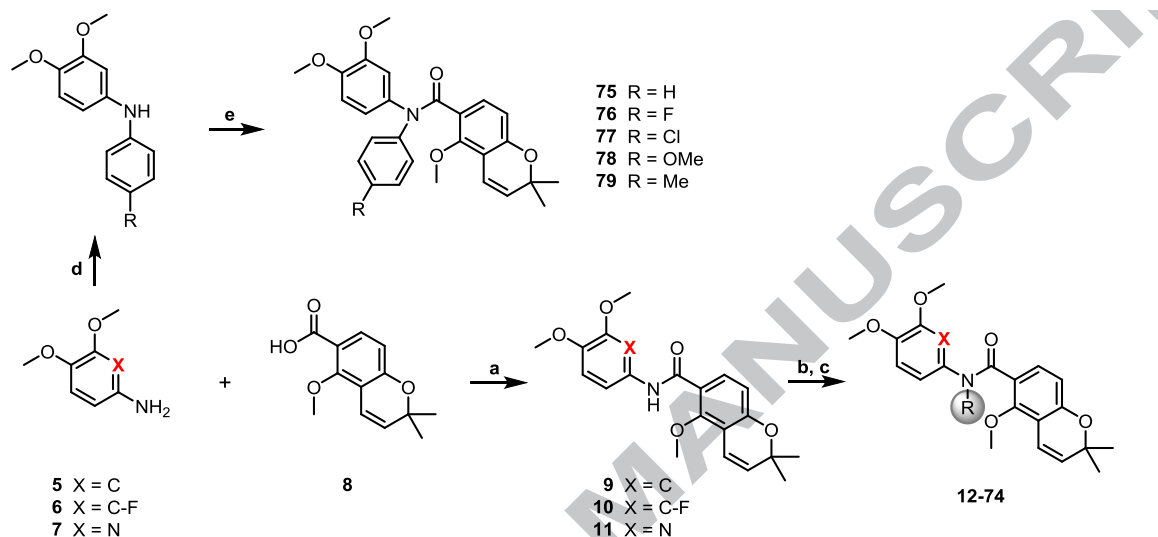
To further optimize the B,C-ring-truncated templates of deguelin as HSP inhibitors, we investigated its amide linker surrogates, represented in template **I** (**Figure 1**). In this study, we demonstrated the structure-activity relationships of the template, in which the A-ring was substituted with 3,4-dimethoxyphenyl, its fluorophenyl or pyridine surrogate, respectively, and the linker was modified with *N*-substituted amide. The synthesized compounds were evaluated for their HIF-1 α inhibitions using western blot assay as the primary screening method. With selected potent inhibitors in the series, we sought to exploit anticancer effect in breast cancer cell lines. In addition, we explored the effect on major clients of HSP90 and performed molecular modeling to identify its mechanism for HSP90 inhibition.

2. Results and discussion

2.1. Chemistry

The syntheses of *N*-substituted B,C-ring truncated deguelin derivatives were represented in **Scheme 1**. For the synthesis of the *N*-alkylated amide compounds (**12-74**), commercially available A-ring amines (**5-7**) were coupled with 2,2-dimethyl-5-methoxy-2*H*-chromene acid (**8**), which was obtained by Pinnick oxidation of previously reported chromene aldehyde³¹ to form the amide intermediates (**9-11**) under general EDC coupling conditions. Their amides were *N*-alkylated with the corresponding halide to provide one part of final products directly or penultimate products, which were deprotected, *O*-methylated or aminated to afford the rest of the final product.

For the synthesis of *N*-phenyl amide compounds (**75-79**), the A-ring amine (**5**) was condensed with halobenzene through Buchwald-Hartwig amination to provide the corresponding diphenylamines. The secondary amines were coupled with the acyl chloride of **8** in the presence of K_2CO_3 to provide the desired final compounds (**75-79**).



X = C	X = C-F	X = N	
12 R = Me	13 R = Me	14 R = Me	49 R = (CH ₂) ₂ -1-pyrrolidine
15 R = (CH ₂) ₂ OTBS	16 R = (CH ₂) ₂ OTBS	17 R = (CH ₂) ₂ OTBS	52 R = (CH ₂) ₂ -1-piperidine
18 R = (CH ₂) ₂ OH	19 R = (CH ₂) ₂ OH	20 R = (CH ₂) ₂ OH	53 R = (CH ₂) ₂ -4-piperidine
21 R = (CH ₂) ₂ OMe	22 R = (CH ₂) ₂ OMe	23 R = (CH ₂) ₂ OMe	56 R = (CH ₂) ₂ -1-morpholine
24 R = (CH ₂) ₂ OBn	25 R = (CH ₂) ₂ OBn	26 R = (CH ₂) ₂ OBn	59 R = (CH ₂) ₂ -1-piperazine
27 R = (CH ₂) ₂ NH ₂	28 R = (CH ₂) ₂ NH ₂	29 R = (CH ₂) ₂ NH ₂	62 R = (CH ₂) ₂ -1-(4-Me)-piperazine
30 R = (CH ₂) ₃ NHBoc	31 R = (CH ₂) ₃ NHBoc	32 R = (CH ₂) ₃ NHBoc	65 R = Bn
33 R = (CH ₂) ₃ NH ₂	34 R = (CH ₂) ₃ NH ₂	35 R = (CH ₂) ₃ NH ₂	66 R = 4-fluorobenzyl
36 R = (CH ₂) ₂ NHMe	37 R = (CH ₂) ₂ NHMe	38 R = (CH ₂) ₂ NHMe	67 R = 4-chlorobenzyl
39 R = (CH ₂) ₂ NMe ₂	40 R = (CH ₂) ₂ NMe ₂	41 R = (CH ₂) ₂ NMe ₂	68 R = 4-methoxybenzyl
44 R = (CH ₂) ₂ NHAc	51 R = (CH ₂) ₂ -1-piperidine	42 R = (CH ₂) ₃ NMe ₂	69 R = 4-methylbenzyl
47 R = (CH ₂) ₂ NHBoc	55 R = (CH ₂) ₂ -1-morpholine	43 R = (CH ₂) ₂ NEt ₂	70 R = 3-fluorobenzyl
50 R = (CH ₂) ₂ -1-piperidine	58 R = (CH ₂) ₂ -1-piperazine	45 R = (CH ₂) ₂ NHAc	71 R = 3-chlorobenzyl
54 R = (CH ₂) ₂ -1-morpholine	61 R = (CH ₂) ₂ -1-(4-Me)-piperazine	46 R = (CH ₂) ₃ NHAc	72 R = CH ₂ -2-pyridinyl
57 R = (CH ₂) ₂ -1-piperazine	64 R = Bn	48 R = (CH ₂) ₂ NHBoc	73 R = CH ₂ -3-pyridinyl
60 R = (CH ₂) ₂ -1-(4-Me)-piperazine			74 R = CH ₂ -4-pyridinyl
63 R = Bn			

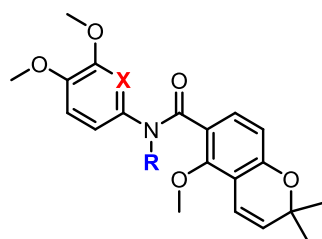
Scheme 1. Reagents and conditions: (a) EDC·HCl, HOBT, NEt₃, 1,4-dioxane, r.t to 50 °C for **9-11**; (b) RX, NaH, DMF, 50-70 °C for **12-17**, **24-26**, **30-32**, **42**, **47**, **63-74**; (c) [TBS deprotection] TBAF, CH₂Cl₂, 0 °C for **18-20**; [O-methylation] NaH, MeI, DMF, 0 °C for **21-23**; [Boc deprotection] TFA, DCM, 0 °C for **33-35**, **53**; [amination: Method A] (i) DPPA, DBU, DMF, 90 °C (ii) Lindlar's catalyst, H₂, MeOH, r.t for **27-29**; [amination: Method B] (i) DMP, CH₂Cl₂, r.t, (ii) NHR₁R₂, ZnCl₂, NaBH₄, CH₂Cl₂, MeOH, r.t for **36-41**, **50-52**, **54-62**; [N-acetylation] Ac₂O, Pyridine, CH₂Cl₂, 0 °C for **44-46**; [N-Boc protection] Boc₂O, CH₂Cl₂, 0 °C for **47-48**; (d) Pd₂(dba)₃, BINAP, NaOtBu, *p*-R-halobenzene, 1,4-dioxane, reflux; (e) (i) **8**, PPh₃, Cl₃CCN, CH₂Cl₂, reflux, (ii) K₂CO₃, 1,4-dioxane, reflux for **75-79**.

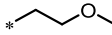
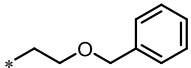
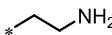
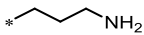
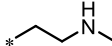
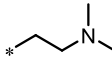
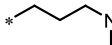
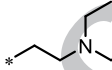
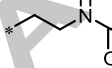
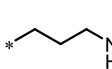
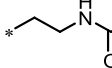
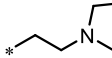
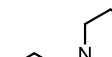
2.2. Structure-activity relationship for HIF-1 α inhibition

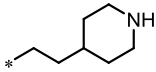
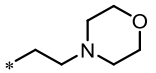
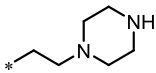
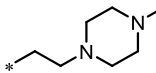
As primary screening for HSP90 inhibitors, the compounds were evaluated for their HIF-1 α inhibition using western blot assay with human nonsmall cell lung carcinoma (H1299) cell lines.²⁸ The H1299 cells were untreated or treated with the compounds at 100 nM for 72 h and subsequently incubated under hypoxic conditions for 12 h. The resulting cell lysates were used for western blot analysis with a monoclonal antibody against HIF-1 α . The results are summarized in **Tables 1-3**, and deguelin (**1**) and **2**, as references, were examined with 64% and 85.3% values, respectively, together with the control (100%).

First, we explored *N*-alkyl amide linker analogues (**Table 1**). Unsubstituted amide linker analogues with different A-regions (**9-11**) were found to be inactive for HIF-1 α inhibition. *N*-Methyl analogues (**12-14**) showed modestly improved inhibition. Whereas *N*-hydroxyethyl analogues (**18-20**) were almost inactive, *N*-methoxyethyl and *N*-benzyloxyethyl analogues (**21-26**) exhibited good inhibition. Surprisingly, the two *N*-aminoethyl analogues (**27, 29**) showed excellent HIF-1 α inhibition, with values of 39.4 and 33.3, respectively, while **28** with the fluorophenyl A-ring was inactive. *N*-Aminopropyl analogue, with a pyridine A-ring (**35**), also exhibited good inhibition. Further modification in **27-29** and **33-35** was explored by incorporating methyl (**36-38**), dimethyl (**39-42**), diethyl (**43**), acetyl (**44-46**) and t-butoxycarbonyl (**47-48**) groups into their amino group. Most analogues with a pyridine A-ring displayed better inhibition than deguelin.

N-cycloalkylethyl analogues (**49-62**), including pyrrolidine, 1-piperidine, 4-piperidine, morpholine, piperazine and *N*-methylpiperazine, were also examined. All showed good inhibition that was similar to that of the corresponding *N*-dimethyl and *N*-diethyl analogues.

Table 1. HIF-1 α inhibitory activities of the synthesized compounds

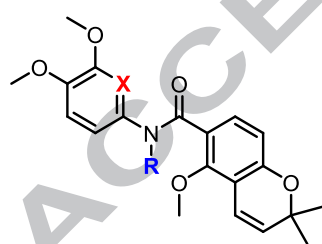
R/X		C-H		C-F		N
-H	9	147 (\pm 30.0)	10	101 (\pm 25.2)	11	88.4 (\pm 19.5)
-Me	12	126 (\pm 16.0)	13	93.1 (\pm 16.0)	14	62.3 (\pm 21.5)
* 	18	133 (\pm 38.1)	19	124 (\pm 16.9)	20	87.9 (\pm 10.5)
* 	21	65.5 (\pm 21.3)	22	59.3 (\pm 23.7)	23	52.5 (\pm 40.3)
* 	24	74.4 (\pm 20.2)	25	65.4 (\pm 22.4)	26	57.2 (\pm 10.3)
* 	27	39.4 (\pm 11.5)	28	147 (\pm 15.2)	29	33.3 (\pm 16.2)
* 	33	100 (\pm 28.1)	34	68.5 (\pm 27.5)	35	45.3 (\pm 10.1)
* 	36	75.9 (\pm 8.87)	37	107 (\pm 30.7)	38	41.2 (\pm 12.8)
* 	39	71.0 (\pm 15.7)	40	53.3 (\pm 14.3)	41	37.9 (\pm 14.0)
* 					42	44.0 (\pm 12.0)
* 					43	64.4 (\pm 14.7)
* 	44	127 (\pm 10.1)			45	58.1 (\pm 20.2)
* 					46	76.6 (\pm 11.3)
* 	47	70.3 (\pm 9.61)			48	57.4 (\pm 24.8)
* 					49	66.0 (\pm 26.4)
* 	50	83.7 (\pm 18.9)	51	54.3 (\pm 16.3)	52	79.7 (\pm 18.4)

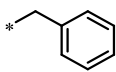
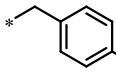
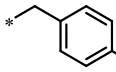
				53	55.2 (±11.5)
	54	117 (±11.1)	55	48.8 (±14.2)	56 60.3 (±21.5)
	57	51.9 (±14.2)	58	54.9 (±19.4)	59 59.4 (±10.2)
	60	61.9 (±19.3)	61	53.7 (±18.8)	62 42.2 (±13.7)

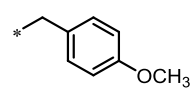
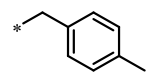
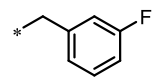
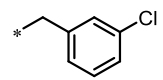
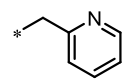
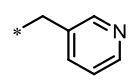
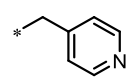
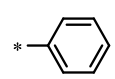
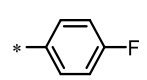
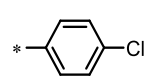
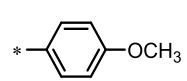
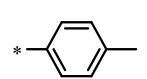
Second, we examined *N*-benzyl and *N*-phenyl amide analogues (**Table 2**).

N-Benzyl analogues (**63-65**) displayed potent inhibition. Of these compounds, pyridine A-ring surrogate (**65**) exhibited excellent inhibition to give a value of 38.6%. Its high potency prompted us to investigate its SAR. The *N*-Benzyl group was modified with 3- or 4-substituted benzyl groups (**66-71**) and isomeric pyridines (**72-74**). Among them, 4-fluorobenzyl (**66**), 4-chlorobenzyl (**67**) and pyridin-4-yl (**74**) analogues exhibited good inhibition. The *N*-Phenyl analogue (**75**) also showed good HIF-1 α inhibition that was better than that of its benzyl surrogate (**63**). However, its substituted analogues (**76-79**) displayed lower inhibition.

Table 2. HIF-1 α inhibitory activities of the synthesized compounds



R/X	C-H	C-F	N
	63 69.8 (±16.0)	64 60.8 (±51.3)	65 38.6 (±22.0)
			66 63.1 (±14.5)
			67 57.6 (±16.5)

	68	77.0 (±16.1)
	69	71.1 (±12.2)
	70	85.7 (±11.4)
	71	80.2 (±15.9)
	72	97.0 (±14.6)
	73	95.8 (±20.9)
	74	55.2 (±15.2)
	75	52.8 (±23.6)
	76	70.2 (±20.0)
	77	81.2 (±22.4)
	78	61.9 (±17.8)
	79	58.9 (±12.2)

Of the tested compounds, we selected 20 compounds having better HIF-1 α inhibition than deguelin and further evaluated their inhibition at a lower concentration (10 nM) to examine the concentration-dependent inhibition (**Table 3**). Among them, 8 compounds (**26, 27, 29, 41, 42, 45, 56, 57**) displayed concentration-dependent inhibition and better inhibition than deguelin at 10 nM.

Table 3. HIF-1 α inhibition of selected compounds

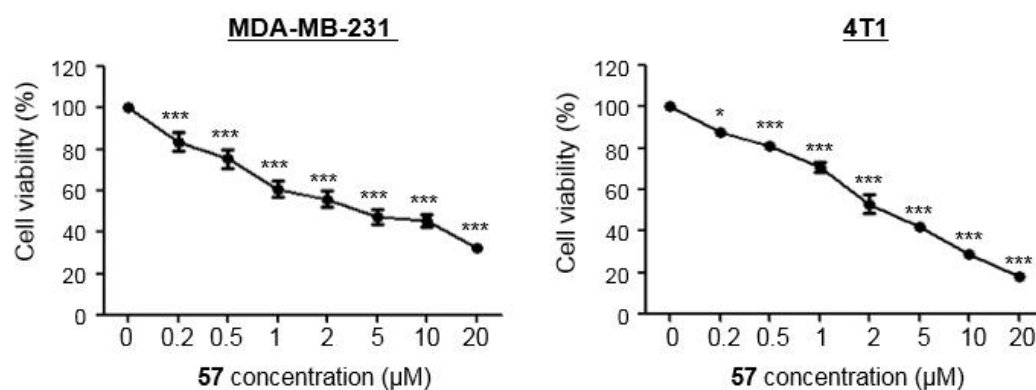
Code	WB (100 nM)	WB (10 nM)
Deguelin	64	94
14	62.3	90.4 (±19.5)
26	57.2	69.3 (±10.1)
27	39.4	62.1 (±9.2)

29	33.3	64.0 (\pm 12.6)
35	45.3	111 (\pm 21.9)
38	41.2	93.0 (\pm 18.2)
40	53.3	97.9 (\pm 14.1)
41	37.9	75.5 (\pm 10.4)
42	44.0	65.6 (\pm 18.5)
45	58.1	66.0 (\pm 11.2)
53	55.2	97.2 (\pm 18.2)
55	48.8	111 (\pm 20.6)
56	60.3	72.9 (\pm 14.8)
57	48.9	60.6 (\pm 12.6)
61	53.7	81.2 (\pm 23.8)
62	42.2	97.2 (\pm 19.8)
65	38.6	83.4 (\pm 14.1)
66	63.1	104 (\pm 16.4)
74	55.2	108 (\pm 12.5)
75	52.8	83.7 (\pm 21.0)

2.3. Antitumor activity

To examine the antitumor activity of HSP90 inhibitors in breast cancer cell lines, we characterized the cytotoxicities of the compounds in **Table 3** in triple-negative breast cancer cell-lines (TNBC). Of those compounds, only compound **57** showed a promising cytotoxic effect in MDA-MB-231 (invasive ductal carcinoma) and 4T1 (murine mammary carcinoma) at a concentration of 10 μ M. To further examine the effects of **57** on cell viability in TNBC, MDA-MB-231 and 4T1 cells were treated with various concentrations of **57** (0.2, 0.5, 1, 2, 5, 10 or 20 μ M) for 72 h. MTS assays revealed **57** (0.2-20 μ M) significantly suppressed cell viability in both MDA-MB-231 and 4T1 cells in a time- and dose-dependent manner (**Figure 2A**). Following exposure to **57** (2-10 μ M) for 72 h, MDA-MB-231 cells exhibited significant morphological changes with concomitant cytoplasmic shrinkage (**Figure 2B**).

A



B

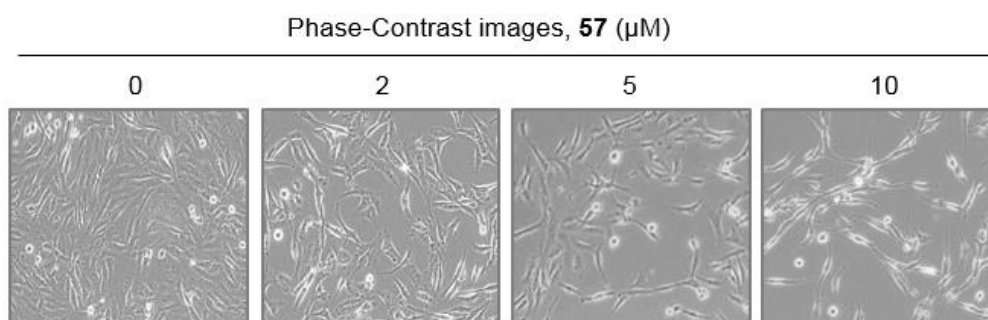


Figure 2. The cytotoxic effect of **57** in triple-negative breast cancer cell-lines

(A) Effect of **57** on cell viability in MDA-MB-231 and 4T1 cells. Cells were treated with various concentrations of **57** (0.2, 0.5, 1, 2, 5, 10 or 20 µM) for and 72 h. Cell viability was determined by MTS assay. The results are presented as mean \pm SEM of at least three independent experiments and analyzed by one-way ANOVA followed by Bonferroni's *post hoc* test (* $p < 0.05$, versus DMSO control). (B) Changes in cellular morphology in MDA-MB-231 cells after **57** (2, 5 or 10 µM) treatment for 72 h as seen through phase contrast microscopy.

2.4. Mechanism study

To identify the mechanism of compound **57** as a HSP90 inhibitor, we examined the influence of **57** on the expression and activation of major clients of HSP90 including AKT (protein kinase B), MEK (mitogen-activated protein kinase kinase) and STAT3 (signal transducer and activator of transcription 3) in MDA-MB-231 cells *in vitro*. Treatment with **57** (5-10 µM, 72 h) resulted in a significant downregulation of AKT, STAT3 and MEK protein content, concomitant with a marked reduction of their phosphorylation (**Figure 3A**). The quantitative data further showed that **57** effectively suppressed activation of these HSP90 clients, as evidenced by a significant reduction in

the ratio of phospho-AKT/total-AKT, phospho-MEK/total-MEK and phospho-STAT3/total-STAT3 in MDA-MB-231 cells (**Figure 3B**). A mitogen-activated protein kinase (MAPK) signaling network has been implicated in diverse aspects of cancer progression, and blockage of the MEK–ERK cascade elicits antitumor activity in many cancer types.³² Exposure to **57** did not affect ERK protein content but significantly hampered its phosphorylation and activity (**Figure 3B**), indicating that this response is attributable to MEK inactivation by **57** challenge. The result revealed that **57** downregulated the expression and phosphorylation of HSP90 client proteins, AKT, ERK and STAT3.

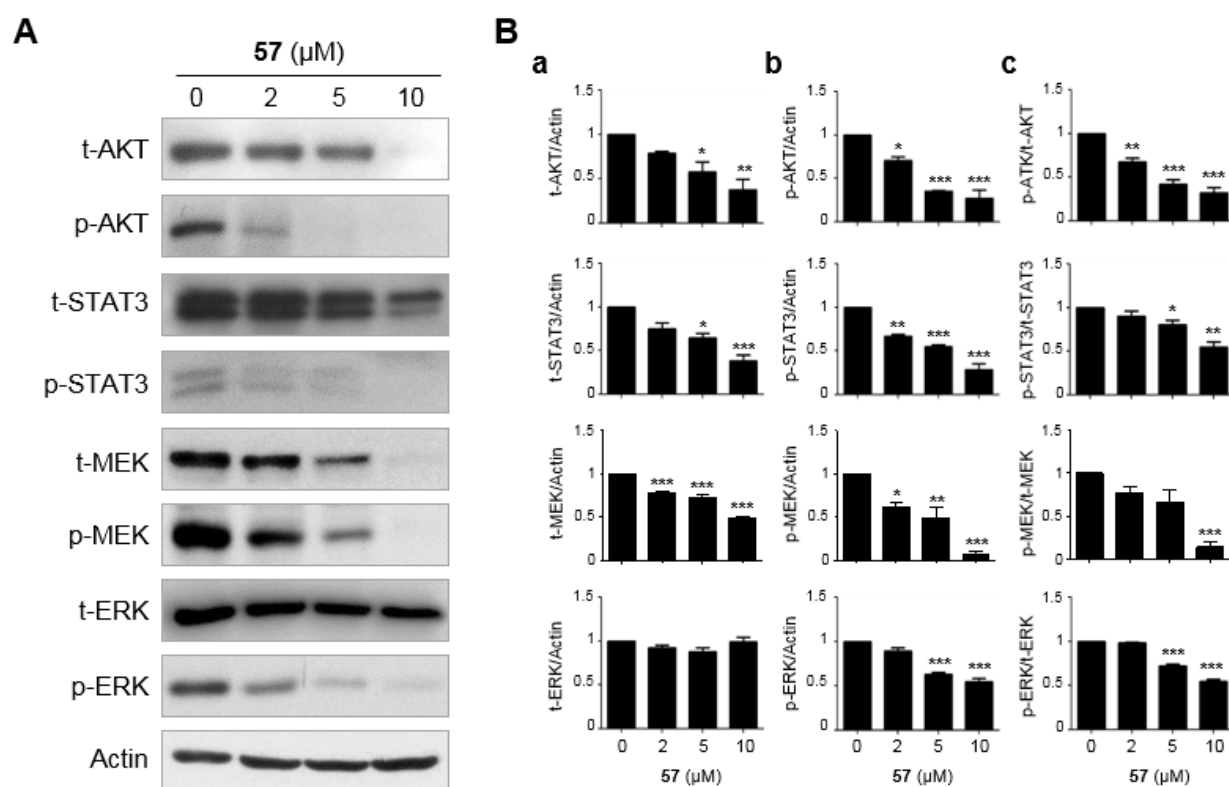


Figure 3. The influence of 57 on AKT/ERK/STAT3 expression and activation

(A) Immunoblot analyses of AKT, phospho-AKT (Ser473), STAT3, phospho-STAT3 (Tyr705), MEK, phospho-MEK (Ser218/222), ERK and phospho-ERK (Thr202/Tyr204) protein expression in MDA-MB-231 cells following **57** (2–10 μM, 72 h) challenge for 72 h. Actin was used as a loading control. (B) Quantitative graphs represent (a) the ratio of total proteins (AKT, -STAT3, -MEK or -ERK)/actin, (b) the ratio of phosphorylated proteins/actin, and (c) the ratio of phosphorylated-/total-proteins, respectively. The results are presented as mean \pm SEM of at least three independent experiments analyzed by one-way ANOVA followed by Bonferroni's *post hoc* test (* $p < 0.05$, versus DMSO control).

2.5. Molecular Modeling

To explore the molecular basis of the interaction between **57** and HSP90, molecular docking analysis was conducted using the Surflex-Dock program.³³ Our previous *h*HSP90 homology model structure^{29,30} was used as the receptor for docking. As expected, **57** binds into the C-terminal ATP-binding cavity, anchoring at the cavity of dimerization interface of HSP90 homodimer with a “T-shape” pose (**Figure 4**). The side-chain amine NH of Lys615(A) forms a hydrogen bond with the methoxy group attached to the 2,2-dimethyl chromene ring, and it concurrently forms a π -cation interaction with 3,4-dimethoxy phenyl ring. The side-chain OH of Ser677(A) forms bidentate hydrogen bonds with 3,4-dimethoxy substituents on the phenyl ring. Upon examining the interaction of **57** with chain B, the two nitrogen atoms in the piperazine ring serve as hydrogen bonding acceptors, interacting with side-chain of Lys615(B) and Ser677(B). Our docking model suggests that compound **57** binds to the interface of the HSP90 homodimer, locking the open conformation of HSP90 homodimer, and therefore prohibiting *N*-terminal dimerization and the formation of the ATP binding pocket.

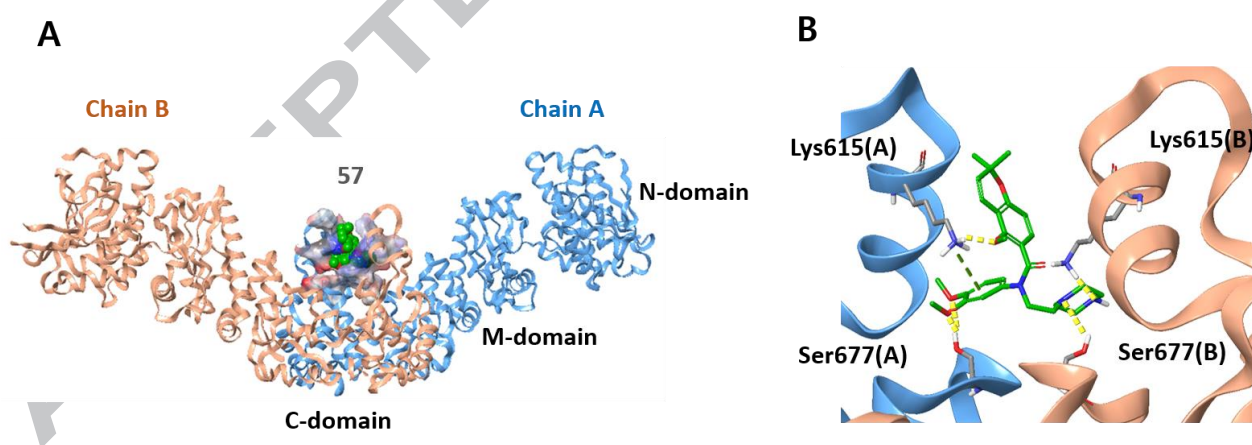


Figure 4. Molecular docking model of 57 bound to the *h*Hsp90 C-terminal domain

(A) Binding site for **57** in the dimerization interface of open state *h*HSP90. Chain A is rendered in blue ribbon, and chain B is orange ribbon. The active site is shown as electrostatic property surface map. Red, blue, and white colored regions correspond to negatively charged, positively charged, and neutral areas, respectively. (B) Docked pose of **57** (carbon in green) in the *h*HSP90 C-terminal ATP binding site. Key amino acid residues within the binding site are rendered in grey capped stick. Hydrogen bonding interactions are depicted as yellow dashed lines and pi-cation interaction is depicted as green dashed lines. A and B indicate chain names.

3. Conclusion

A series of the B,C-ring truncated surrogates of deguelin with *N*-substituted amide linkers were investigated as HSP90 inhibitors by examining their HIF-1 α inhibition as a primary screening method. The structure-activity relationship of the template was investigated by alkylation, benzylation and phenylation on the nitrogen of the amide linker in the template. Among 68 compounds synthesized, 8 compounds displayed better inhibition than deguelin at 100 and 10 nM with concentration-dependent inhibition. The selected compounds were screened for antitumor activity in triple-negative breast cancer cell-lines, and of those, compound **57** showed potent cytotoxicity in MDA-MB-231 and 4T1 cells in a time- and dose-dependent manner. The mechanistic study indicated that **57** downregulated expression and phosphorylation of major client proteins of HSP90 including AKT, ERK and STAT3, revealing that it induced antitumor activity by inhibiting the function of HSP90. The docking study of **57** with the *h*HSP90 C-terminal ATP-binding site indicated that **57** binds with a T-shape pose to the C-terminal ATP-binding pocket in the open conformation of *h*HSP90 homodimer by hydrogen bonding and pi-cation interactions. Overall, compound **57** is a potential antitumor agent for triple-negative breast cancer, and it acts as a HSP90 C-terminal inhibitor.

4. Experimental

4.1. Chemistry

4.1.1. General

All chemical reagents were commercially available. Melting points were determined on a Büchi Melting Point B-540 apparatus and are uncorrected. Silica gel column chromatography was performed on silica gel 60, 230-400 mesh, Merck. ¹H NMR spectra were recorded on a JEOL JNM-LA 300 and a Bruker Avance 500 at 500 MHz. Chemical shifts are reported in ppm units with Me₄Si as a reference standard. Mass spectra were recorded on a VG Trio-2 GC-MS and 6460 Triple Quad LC/MS.

4.1.2. General procedure

4.1.2.1. EDC coupling. To a solution of **8** (1.0 mmol) and appropriate aniline (**5-6**, 1.0 eq.) in 1,4-dioxane, 1-ethyl-3-(3-dimethylaminopropyl)carbodiimide (EDC-HCl, 1.3 eq.), hydroxybenzotriazole (HOBT, 1.3 eq.) and triethylamine (1.3 eq.) were added and stirred at 50 °C for 15 h. After completion, the reaction mixture was diluted with H₂O and extracted with EtOAc. The combined organic layers was washed with brine three times, dried over MgSO₄ and concentrated *in vacuo*. The residue was purified by silica gel column chromatography to obtain the desired compounds.

4.1.2.2. N-alkylation. To a solution of amide compound (**9-11**, 1.0 eq.) in DMF, sodium hydride (NaH, 1.5 eq.) was added at 0 °C and stirred for 30 min. The appropriate alkylhalides (**S1-S3**, 2.0 eq.) dissolved in DMF were added dropwise and stirred for 1 h. The reaction mixture was quenched by dropwise addition of water at 0 °C and extracted with EtOAc, washed with brine several times, dried over MgSO₄, and concentrated *in vacuo*. The residue was purified by silica gel column chromatography to obtain the desired compounds.

4.1.2.3. Silyl deprotection. To a solution of compound **15-17** (1.0 eq.) in DCM, TBAF 1 M in THF (1.2 eq.) was added at 0 °C and stirred for 2 h at room temperature. The reaction mixture was quenched with H₂O and extracted with EtOAc. The organic layer was washed with brine, dried over MgSO₄, and concentrated *in vacuo*. The residue was purified by silica gel column chromatography to obtain the desired compounds.

4.1.2.4. O-Methylation. An oven-dried round bottom flask was charged with compounds **18-20** (1.0 eq.), sodium hydride (1.2 eq.) and DMF. The mixture was stirred at 0 °C, and iodomethane (1.0 eq.) was added dropwise. The mixture was warmed to room temperature for 1 h. The reaction was quenched by the addition of water and extracted twice with EtOAc. The combined organic layer was washed with brine, dried over MgSO₄, filtered and concentrated *in vacuo*. The crude mixture was purified by silica gel column chromatography to afford the desired product.

4.1.2.5. Boc deprotection. To a solution of *N*-Boc protected compounds (**30-32**, 1.0 eq.) in DCM, TFA (1.2 eq.) was added dropwise at 0 °C and stirred for 1 h at room temperature. Then, the reaction mixture was quenched with saturated NaHCO₃ solution and extracted with EtOAc. The organic layer was washed with brine, dried over MgSO₄, and concentrated *in vacuo*. The residue was purified by flash column chromatography on *silica* gel to afford the desired product.

4.1.2.6. Amination

Method A: To a solution of compound **18-20** (1.0 eq.) in DMF, 1,8-diazabicyclo(5.4.0)undec-7-ene (DBU, 1.2 eq.) and diphenylphosphoryl azide (DPPA, 1.2 eq.) were added dropwise, and the reaction mixture was stirred for 15 h at 80 °C. After completion, the mixture was cooled down to room temperature, quenched with H₂O and extracted with EtOAc. The combined organic layer was washed with brine, dried over MgSO₄, filtered and concentrated *in vacuo*. The crude mixture was purified by silica gel column chromatography to afford the desired azide intermediate. To azide intermediates in MeOH, Lindlar catalyst (0.1 eq.) was added and stirred for 1 h under H₂ atmosphere at room temperature. After completion, the mixture was filtered through a celite filter, and the filtrate was concentrated *in vacuo*. The residue was purified by flash column chromatography on silica gel to afford the desired product.

Method B: To a solution of compound **18-20** (1.0 eq.) in DCM, Dess–Martin periodinane (DMP, 1.0 eq.) was added and stirred for 1 h at room temperature. After completion, the reaction mixture was neutralized with sodium bicarbonate solution (NaHCO₃ sat.) and extracted with DCM. The combined organic layer was washed with brine, dried over MgSO₄, filtered and concentrated *in vacuo*. The crude mixture was purified by silica gel column chromatography to afford the desired aldehyde intermediate. To a solution of the aldehyde (1.0 eq.) in DCM, ZnCl₂ (1.2 eq.) and NHR₁R₂ or its salt (1.2 eq.) was added at 0 °C and stirred for 15 h at room temperature. Then, the reaction mixture was concentrated and redissolved in MeOH. NaBH₄ (2.0 eq.) was added to the reaction mixture at 0 °C and stirred for 1 h at room temperature. After completion, the reaction mixture was quenched with

H₂O and extracted with EtOAc. The combined organic layer was washed with brine, dried over MgSO₄, filtered and concentrated *in vacuo*. The crude mixture was purified by silica gel column chromatography to afford the desired product.

4.1.2.7. N-Acetylation. To a solution of alkyl amine in DCM, pyridine (1.0 eq.) and acyl anhydride (1.0 eq.) were added dropwise at 0 °C and stirred for 1 h at room temperature. After completion, the reaction mixture was neutralized with saturated NaHCO₃ solution and extracted with DCM. The combined organic layer was washed with brine, dried over MgSO₄, filtered and concentrated *in vacuo*. The crude mixture was purified by silica gel column chromatography to afford the desired product.

4.1.2.8. N-tert-Butoxycarbonylation. To a solution of alkyl amine (1.0 eq.) in DCM, triethylamine (2.0 eq.) and tert-butyloxycarbonyl anhydride (3 eq.) was added and stirred for 3 h at room temperature. After completion, the reaction mixture was quenched with H₂O and extracted with DCM. The combined organic layer was washed with brine, dried over MgSO₄, filtered and concentrated *in vacuo*. The crude mixture was purified by silica gel column chromatography to afford the desired product.

4.1.2.9. Buchwald reaction. To a solution of aromatic halide compound (1.0 eq.) in 1,4-dioxane, appropriate aniline (1.0 eq.), Pd₂(dba)₃ (0.1 eq.), BINAP (0.1 eq.), NaOtBu (2.5 eq.) were added and refluxed overnight. After completion, the mixture was filtered through a celite filter, and the filtrate was washed with brine, dried over MgSO₄, and concentrated *in vacuo*. The residue was purified by flash column chromatography on silica gel to afford the desired secondary amine intermediate.

4.1.2.10. Acylation and coupling. To a solution of carboxylic acid (**8**, 1.0 eq.) in DCM, PPh₃ (1.1 eq.), Cl₃CCN (1.1 eq.) were added and refluxed for 2 h. After completion, the reaction mixture was concentrated *in vacuo* to obtain 5-methoxy-2,2-dimethyl-2H-chromene-6-carbonyl chloride. The appropriate amine intermediates (1.0 eq.) in 1,4-dioxane were added with K₂CO₃ (3.0 eq.) and

carbonyl chloride, and the solution was refluxed for 15 h. After completion, the reaction mixture was quenched with H₂O and extracted with DCM. The combined organic layer was washed with brine, dried over MgSO₄, filtered and concentrated *in vacuo*. The crude mixture was purified by silica gel column chromatography to afford the desired product.

4.1.3. Chemical Spectra

4.1.3.1. *N*-(3,4-Dimethoxyphenyl)-5-methoxy-2,2-dimethyl-2H-chromene-6-carboxamide (9).

Yield = 80%, white solid; ¹H-NMR (CDCl₃, 300 MHz) δ 9.60 (s, 1H), 7.94 (d, *J* = 8.6 Hz, 1H), 7.61 (d, *J* = 2.2 Hz, 1H), 6.93 (dd, *J* = 2.4, 8.6 Hz, 1H), 6.82 (d, *J* = 8.6 Hz, 1H), 6.70 (d, *J* = 9.0 Hz, 1H), 6.58 (d, *J* = 10.1 Hz, 1H), 5.71 (d, *J* = 10.1 Hz, 1H), 3.91 (s, 3H), 3.86 (s, 3H), 3.86 (s, 3H), 1.44 (s, 6H); HR-MS (FAB) Calcd for C₂₁H₂₄NO₅ [M + H]⁺ 370.1654, found: 370.1651.

4.1.3.2. *N*-(2-Fluoro-3,4-dimethoxyphenyl)-5-methoxy-2,2-dimethyl-2H-chromene-6-carboxamide (10).

Yield = 65%, white solid, mp = 117-118 °C; ¹H-NMR (CDCl₃, 400 MHz) δ 10.05 (s, 1H), 8.11 (t, *J* = 8.7 Hz, 1H), 7.97 (d, *J* = 8.6 Hz, 1H), 6.68 (m, 2H), 6.58 (d, *J* = 10.0 Hz, 1H), 5.70 (d, *J* = 10.0 Hz, 1H), 3.94 (s, 3H), 3.86 (s, 3H), 3.81 (s, 3H), 1.44 (s, 6H); HRMS (FAB) calcd for C₂₁H₂₃FNO₅ [M + H]⁺ 388.1560, found: 388.1559.

4.1.3.3. *N*-(5,6-Dimethoxypyridin-2-yl)-5-methoxy-2,2-dimethyl-2H-chromene-6-carboxamide (11).

Yield = 55%, pale yellow solid, mp = 127-128 °C; ¹H-NMR (CDCl₃, 300 MHz) δ 9.99 (s, 1H), 7.96 (d, *J* = 8.6 Hz, 1H), 7.88 (d, *J* = 8.4 Hz, 1H), 7.13 (d, *J* = 8.4 Hz, 1H), 6.71 (d, *J* = 8.6 Hz, 1H), 6.61 (d, *J* = 10.1 Hz, 1H), 5.73 (d, *J* = 9.9 Hz, 1H), 3.99 (s, 3H), 3.91 (s, 3H), 3.88 (s, 3H), 1.47 (s, 6H); HRMS (FAB) calcd for C₂₀H₂₃N₂O₅ [M + H]⁺ 371.1607, found: 371.1609.

4.1.3.4. *N*-(3,4-Dimethoxyphenyl)-5-methoxy-*N*,2,2-trimethyl-2H-chromene-6-carboxamide (12).

Yield = 85%, colorless oil; ¹H NMR (CDCl₃, 300 MHz) δ 6.60 - 6.47 (m, 6H), 5.57 (d, *J* = 9.7 Hz,

1H), 3.85 (s, 3H), 3.77 (s, 3H), 3.66 (s, 3H), 3.42 (s, 3H), 1.34 (s, 6H); HR-MS (ESI) m/z calcd for $C_{22}H_{26}NO_5$ $[M + H]^+$ 384.1805, found 384.1807.

4.1.3.5. *N-(2-Fluoro-3,4-dimethoxyphenyl)-5-methoxy-N,2,2-trimethyl-2H-chromene-6-carboxamide (13)*. Yield = 90%, pale yellow oil; 1H -NMR ($CDCl_3$, 300 MHz) δ 6.92 (d, $J = 8.3$ Hz, 1H), 6.71 (t, $J = 8.8$ Hz, 1H), 6.40 (m, 3H), 5.57 (d, $J = 10.1$ Hz, 1H), 3.83 (s, 3H), 3.82 (s, 3H), 3.77 (s, 3H), 3.38 (s, 3H), 1.35 (s, 6H); HRMS (FAB) calcd for $C_{22}H_{25}FNO_5$ $[M + H]^+$ 402.1717, found: 402.1721.

4.1.3.6. *N-(5,6-Dimethoxypyridin-2-yl)-5-methoxy-N,2,2-trimethyl-2H-chromene-6-carboxamide (14)*. Yield = 90%, pale yellow oil; 1H -NMR ($CDCl_3$, 300 MHz) δ 6.87 (m, 2H), 6.50 (m, 2H), 6.40 (d, $J = 8.4$ Hz, 1H), 5.60 (d, $J = 9.9$ Hz, 1H), 3.88 (s, 3H), 3.86 (s, 3H), 3.80 (s, 3H), 3.47 (s, 3H), 1.39 (s, 6H); HRMS (FAB) calcd for $C_{21}H_{25}N_2O_5$ $[M + H]^+$ 385.1763, found: 385.1768.

4.1.3.7. *N-(3,4-Dimethoxyphenyl)-N-(2-hydroxyethyl)-5-methoxy-2,2-dimethyl-2H-chromene-6-carboxamide (18)*. Yield = 70%, yellow oil; 1H -NMR ($CDCl_3$, 300 MHz) δ 6.77 (d, $J = 8.3$ Hz, 1H), 6.68 (m, 3H), 6.44 (d, $J = 9.9$ Hz, 1H), 6.34 (d, $J = 8.4$ Hz, 1H), 5.59 (d, $J = 9.9$ Hz, 1H), 4.09 (t, $J = 5.1$ Hz, 2H), 3.88 (m, 5H), 3.79 (s, 3H), 3.71 (s, 3H), 3.27 (bs, 1H), 1.36 (s, 6H); HRMS (FAB) calcd for $C_{23}H_{27}NO_6$ $[M]^+$ 413.1838, found: 413.1835.

4.1.3.8. *N-(2-Fluoro-3,4-dimethoxyphenyl)-N-(2-hydroxyethyl)-5-methoxy-2,2-dimethyl-2H-chromene-6-carboxamide (19)*. Yield = 70%, pale yellow oil; 1H -NMR (CD_3OD , 300 MHz) δ 6.95-6.90 (m, 2H), 6.66-6.59 (m, 1H), 6.40 (d, $J = 10.6$ Hz, 1H), 6.37 (d, $J = 8.6$ Hz, 1H), 5.64 (d, $J = 9.9$ Hz, 1H), 4.20 (m, 2H), 3.79 (s, 3H), 3.76 (s, 3H), 3.70 (s, 3H), 3.69-3.63 (m, 2H), 1.31 (s, 6H); HRMS (FAB) calcd for $C_{23}H_{27}FNO_6$ $[M + H]^+$ 432.1822, found: 432.1825.

4.1.3.9. *N*-(5,6-Dimethoxypyridin-2-yl)-*N*-(2-hydroxyethyl)-5-methoxy-2,2-dimethyl-2*H*-chromene-6-carboxamide (**20**). Yield = 65%, pale yellow oil; ¹H-NMR (CDCl₃, 400 MHz) δ 6.84 (m, 2H), 6.62 (m, 1H), 6.50 (d, *J* = 10.0 Hz, 1H), 6.37 (d, *J* = 8.3 Hz, 1H), 5.60 (d, *J* = 9.6 Hz, 1H), 4.09 (m, 2H), 3.90 (s, 3H), 3.83 (s, 3H), 3.79 (s, 3H), 1.38 (s, 6H); HRMS (FAB) calcd for C₂₂H₂₆N₂O₆ [M]⁺ 414.1791, found 414.1792.

4.1.3.10. *N*-(3,4-Dimethoxyphenyl)-5-methoxy-*N*-(2-methoxyethyl)-2,2-dimethyl-2*H*-chromene-6-carboxamide (**21**). Yield = 80%, pale yellow oil; ¹H-NMR (CDCl₃, 300 MHz) δ 6.77-6.61 (m, 4H), 6.44 (d, *J* = 9.9 Hz, 1H), 6.32(d, *J* = 8.4 Hz, 1H), 5.58 (d, *J* = 9.9 Hz, 1H), 4.04 (t, *J* = 5.7 Hz, 2H), 3.88 (s, 3H), 3.79 (s, 3H), 3.70 (s, 3H), 3.66 (t, *J* = 5.7 Hz, 2H), 3.39 (s, 3H), 1.35 (s, 6H); HRMS (FAB) calcd for C₂₄H₃₀NO₆ [M + H]⁺ 428.2073, found: 428.2077.

4.1.3.11. *N*-(2-Fluoro-3,4-dimethoxyphenyl)-5-methoxy-*N*-(2-methoxyethyl)-2,2-dimethyl-2*H*-chromene-6-carboxamide (**22**). Yield = 60%, pale yellow oil; ¹H-NMR (CDCl₃, 300 MHz) δ 6.90 (d, *J* = 8.7 Hz, 1H), 6.83 (t, *J* = 8.4 Hz, 1H), 6.71 (d, *J* = 9.9 Hz, 2H), 6.33 (d, *J* = 8.4 Hz, 1H), 5.53 (d, *J* = 10.2 Hz, 1H), 4.31-4.27 (m, 2H), 3.82 (s, 3H), 3.75 (s, 6H), 3.66-3.55 (m, 2H), 3.32 (s, 3H), 1.31 (s, 6H); HRMS (FAB) calcd for C₂₄H₂₉FNO₆ [M + H]⁺ 446.1979, found: 446.1982.

4.1.3.12. *N*-(5,6-Dimethoxypyridin-2-yl)-5-methoxy-*N*-(2-methoxyethyl)-2,2-dimethyl-2*H*-chromene-6-carboxamide (**23**). Yield = 85%, pale yellow solid, mp = 60-61 °C; ¹H-NMR (CDCl₃, 400 MHz) δ 7.27 (m, 1H), 6.87 (m, 3H), 6.47 (d, *J* = 8.2 Hz, 1H), 5.59 (m, 1H), 4.19 (m, 2H), 3.88 (s, 3H), 3.86 (s, 3H), 3.82 (s, 3H), 3.68 (m, 2H), 3.45 (s, 3H), 1.44 (s, 6H); HRMS (FAB) calcd for C₂₃H₂₉N₂O₆ [M + H]⁺ 429.2026, found 429.2018.

4.1.3.13. *N*-(2-(Benzyloxy)ethyl)-*N*-(3,4-dimethoxyphenyl)-5-methoxy-2,2-dimethyl-2*H*-chromene-6-carboxamide (**24**). Yield = 70%, pale yellow oil; ¹H-NMR (CDCl₃, 300 MHz) δ 7.35-

7.26 (m, 5H), 6.72 (m, 2H), 6.60 (m, 2H), 6.44 (d, $J = 9.9$ Hz, 1H), 6.31 (d, $J = 8.4$ Hz, 1H), 5.58 (d, $J = 9.9$ Hz, 1H), 4.56 (s, 2H), 4.11 (m, 3H), 3.85 (s, 3H), 3.81 (t, $J = 5.5$ Hz, 2H), 3.77 (s, 3H), 3.56 (s, 3H), 1.35 (s, 6H); HRMS (FAB) calcd for $C_{30}H_{34}NO_6^+$ $[M + H]^+$ 504.2386, found: 504.2383.

4.1.3.14. *N*-(2-(Benzyloxy)ethyl)-*N*-(2-fluoro-3,4-dimethoxyphenyl)-5-methoxy-2,2-dimethyl-2H-chromene-6-carboxamide (25). Yield = 70%, pale yellow oil; 1H -NMR ($CDCl_3$, 300 MHz) δ 7.33-7.26 (m, 5H), 6.90 (dd, $J = 8.1, 0.9$ Hz, 1H), 6.79 (t, $J = 9.0$ Hz, 1H), 6.42-6.33 (m, 3H), 5.54 (d, $J = 9.9$ Hz, 1H), 4.51-4.31 (m, 4H), 3.74 (s, 3H), 3.73 (s, 3H), 3.72 (s, 3H), 3.72-3.66 (m, 2H), 1.31 (s, 3H), 1.30 (s, 3H); HRMS (FAB) calcd for $C_{30}H_{33}FNO_6^+$ $[M + H]^+$ 522.2292, found: 522.2291.

4.1.3.15. *N*-(2-(Benzyloxy)ethyl)-*N*-(5,6-dimethoxypyridin-2-yl)-5-methoxy-2,2-dimethyl-2H-chromene-6-carboxamide (26). Yield = 82%, pale yellow solid, mp = 69-70 °C; 1H -NMR ($CDCl_3$, 400 MHz) δ 7.39 (m, 1H), 7.32 (m, 5H), 6.83 (m, 2H), 6.50 (d, $J = 10.0$ Hz, 1H), 6.36 (d, $J = 8.2$ Hz, 1H), 5.59 (d, $J = 10.4$ Hz, 1H), 4.49 (m, 2H), 4.26 (m, 2H), 3.85 (s, 3H), 3.82 (s, 3H), 3.76 (s, 3H), 3.61 (m, 2H), 1.38 (s, 6H); HRMS (FAB) calcd for $C_{29}H_{33}N_2O_6^+$ $[M + H]^+$ 505.2339, found 505.2334.

4.1.3.16. *N*-(2-Aminoethyl)-*N*-(3,4-dimethoxyphenyl)-5-methoxy-2,2-dimethyl-2H-chromene-6-carboxamide (27). Yield = 82%, pale yellow solid, mp = 69-70 °C; 1H -NMR ($CDCl_3$, 400 MHz) δ 7.39 (m, 1H), 7.32 (m, 5H), 6.83 (m, 2H), 6.50 (d, $J = 10.0$ Hz, 1H), 6.36(d, $J = 8.2$ Hz, 1H), 5.59 (d, $J = 10.4$ Hz, 1H), 4.49 (m, 2H), 4.26 (m, 2H), 3.85 (s, 3H), 3.82 (s, 3H), 3.76 (s, 3H), 3.61 (m, 2H), 1.38 (s, 6H); HRMS (FAB) calcd for $C_{23}H_{29}N_2O_5^+$ $[M + H]^+$ 413.2339, found 413.2334.

4.1.3.17. *N*-(2-Aminoethyl)-*N*-(2-fluoro-3,4-dimethoxyphenyl)-5-methoxy-2,2-dimethyl-2H-chromene-6-carboxamide (28). Yield = 70%, pale yellow solid, mp = 105-106 °C; 1H -NMR ($CDCl_3$, 300 MHz) δ 6.97 (d, $J = 8.2$ Hz, 1H), 6.88 (t, $J = 8.8$ Hz, 1H), 6.62 (dd, $J = 9.0, 1.8$ Hz, 1H), 6.40 (d, $J = 9.7$ Hz, 1H), 6.87 (d, $J = 7.9$ Hz, 1H), 5.66 (d, $J = 10.1$ Hz, 1H), 4.06 (m, 2H), 3.78 (s, 3H), 3.76

(s, 3H), 3.71 (s, 3H), 2.85 (t, $J = 6.8$ Hz, 2H), 1.31 (s, 6H); HRMS (FAB) calcd for $C_{23}H_{28}FN_2O_5$ [$M + H$]⁺ 431.1982, found: 431.1979.

4.1.3.18. *N*-(2-Aminoethyl)-*N*-(5,6-dimethoxypyridin-2-yl)-5-methoxy-2,2-dimethyl-2H-chromene-6-carboxamide (**29**). Yield = 70%, pale yellow solid, mp = 105-106 °C; ¹H-NMR (CDCl₃, 300 MHz) δ 6.97 (d, $J = 8.2$ Hz, 1H), 6.88 (t, $J = 8.8$ Hz, 1H), 6.62 (dd, $J = 9.0, 1.8$ Hz, 1H), 6.40 (d, $J = 9.7$ Hz, 1H), 6.87 (d, $J = 7.9$ Hz, 1H), 5.66 (d, $J = 10.1$ Hz, 1H), 4.06 (m, 2H), 3.78 (s, 3H), 3.76 (s, 3H), 3.71 (s, 3H), 2.85 (t, $J = 6.8$ Hz, 2H), 1.31 (s, 6H); HRMS (FAB) calcd for $C_{22}H_{28}N_3O_5$ [$M + H$]⁺ 414.1982, found: 414.1979.

4.1.3.19. *N*-(3-Aminopropyl)-*N*-(3,4-dimethoxyphenyl)-5-methoxy-2,2-dimethyl-2H-chromene-6-carboxamide (**33**). Yield = 70%, pale yellow oil; ¹H-NMR (CD₃OD, 300 MHz) δ 6.80-6.69 (m, 4H), 6.46 (d, $J = 9.9$ Hz, 1H), 6.32 (d, $J = 8.4$ Hz, 1H), 5.71 (d, $J = 10.1$ Hz, 1H), 4.03 (t, $J = 6.6$ Hz, 2H), 3.85 (s, 3H), 3.72 (s, 3H), 3.67 (s, 3H), 3.10 (t, $J = 7.3$ Hz, 2H), 1.97-1.92 (m, 2H), 1.33 (s, 6H); HRMS (FAB) calcd for $C_{24}H_{31}N_2O_5$ [$M + H$]⁺ 427.2233, found: 427.2221.

4.1.3.20. *N*-(3-Aminopropyl)-*N*-(2-fluoro-3,4-dimethoxyphenyl)-5-methoxy-2,2-dimethyl-2H-chromene-6-carboxamide (**34**). Yield = 70%, pale yellow oil; ¹H-NMR (CD₃OD, 300 MHz) δ 6.92-6.87 (m, 2H), 6.67 (d, $J = 9.0$ Hz, 1H), 6.41 (d, $J = 9.9$ Hz, 1H), 6.36 (d, $J = 8.6$ Hz, 1H), 5.68 (d, $J = 9.9$ Hz, 1H), 3.91 (m, 2H), 3.80 (s, 3H), 3.77 (s, 3H), 3.70 (s, 3H), 3.12-3.07 (m, 2H), 1.93 (m, 2H), 1.32 (s, 6H); HRMS (FAB) calcd for $C_{24}H_{30}FN_2O_5$ [$M + H$]⁺ 445.2139, found: 445.2130.

4.1.3.21. *N*-(3-Aminopropyl)-*N*-(5,6-dimethoxypyridin-2-yl)-5-methoxy-2,2-dimethyl-2H-chromene-6-carboxamide (**35**). Yield = 45%, yellow oil; ¹H-NMR (CDCl₃, 300 MHz) δ 6.78 (m, 2H), 6.46 (d, $J = 10.0$ Hz, 1H), 6.41 (d, $J = 8.0$ Hz, 1H), 6.33 (d, $J = 8.4$ Hz, 1H), 5.61 (d, $J = 10.0$

Hz, 1H), 4.16 (m, 2H), 3.87 (s, 3H), 3.83 (s, 3H), 3.77 (s, 3H), 3.16 (m, 2H), 2.00 (m, 4H), 1.37 (s, 6H); HRMS (FAB) calcd for C₂₃H₃₀N₃O₅ [M + H]⁺ 428.2185, found 428.2185.

4.1.3.22. *N*-(3,4-Dimethoxyphenyl)-5-methoxy-2,2-dimethyl-*N*-(2-(methylamino)ethyl)-2H-chromene-6-carboxamide (**36**). Yield = 45%, pale yellow oil; ¹H-NMR (CD₃OD, 300 MHz) δ 6.88 (d, *J* = 8.4 Hz, 1H), 6.78-6.70 (m, 3H), 6.44 (d, *J* = 10.1 Hz, 1H), 6.34 (d, *J* = 8.4 Hz, 1H), 5.68 (d, *J* = 10.1 Hz, 1H), 4.07 (t, *J* = 6.6 Hz, 2H), 3.83 (s, 3H), 3.72 (s, 3H), 3.67 (s, 3H), 2.94 (t, *J* = 6.6 Hz, 2H), 2.51 (s, 3H), 1.32 (s, 6H); HRMS (FAB) calcd for C₂₄H₃₁N₂O₅ [M + H]⁺ 427.2233, found: 427.2247.

4.1.3.23. *N*-(2-Fluoro-3,4-dimethoxyphenyl)-5-methoxy-2,2-dimethyl-*N*-(2-(methylamino)-ethyl)-2H-chromene-6-carboxamide (**37**). Yield = 70%, pale yellow solid, mp = 84-85 °C; ¹H-NMR (CDCl₃, 300 MHz) δ 6.99 (d, *J* = 7.7 Hz, 1H), 6.87 (t, *J* = 8.8 Hz, 1H), 6.63 (dd, *J* = 9.0, 1.8 Hz, 1H), 6.40 (d, *J* = 9.9 Hz, 1H), 6.38 (d, *J* = 8.1 Hz, 1H), 5.67 (d, *J* = 9.9 Hz, 1H), 4.08-3.87 (m, 2H), 3.78 (s, 3H), 3.76 (s, 3H), 3.72 (s, 3H), 3.03 (t, 2H, *J* = 6.6 Hz), 2.60 (s, 3H), 1.31 (s, 6H); HRMS (FAB) calcd for C₂₄H₃₀FN₂O₅ [M + H]⁺ 445.2139, found: 445.2146.

4.1.3.24. *N*-(5,6-Dimethoxypyridin-2-yl)-5-methoxy-2,2-dimethyl-*N*-(2-(methylamino)ethyl)-2H-chromene-6-carboxamide (**38**). Yield = 80%, pale yellow solid, mp = 88-89 °C; ¹H-NMR (CD₃OD, 300 MHz) δ 7.03 (d, *J* = 7.9 Hz, 1H), 6.91 (d, *J* = 8.2 Hz, 1H), 6.59 (m, 1H), 6.47 (d, *J* = 9.9 Hz, 1H), 6.38 (d, *J* = 8.2 Hz, 1H), 5.69 (d, *J* = 9.9 Hz, 1H), 4.10 (t, *J* = 6.6 Hz, 2H), 3.84 (s, 3H), 3.81 (s, 3H), 3.74 (s, 3H), 2.88 (t, *J* = 6.6 Hz, 2H), 2.43 (s, 3H), 1.35 (s, 6H); HRMS (FAB) calcd for C₂₃H₃₀N₃O₅ [M + H]⁺ 428.2185, found: 428.2186.

4.1.3.25. *N*-(3,4-Dimethoxyphenyl)-*N*-(2-(dimethylamino)ethyl)-5-methoxy-2,2-dimethyl-2H-chromene-6-carboxamide (**39**). Yield = 45%, pale yellow oil; ¹H-NMR (CD₃OD, 300 MHz) δ 6.84

(d, $J = 8.4$ Hz, 1H), 6.75 (m, 3H), 6.44 (d, $J = 9.9$ Hz, 1H), 6.33 (d, $J = 8.0$ Hz, 1H), 5.67 (d, $J = 9.9$ Hz, 1H), 4.02 (m, 2H), 3.83 (s, 3H), 3.73 (s, 3H), 3.67 (s, 3H), 2.62 (m, 2H), 2.33 (s, 6H), 1.32 (s, 6H); HRMS (FAB) calcd for $C_{25}H_{33}N_2O_5$ $[M + H]^+$ 441.2389, found: 441.2380.

4.1.3.26. *N*-(2-(Dimethylamino)ethyl)-*N*-(2-fluoro-3,4-dimethoxyphenyl)-5-methoxy-2,2-dimethyl-2H-chromene-6-carboxamide (**40**). Yield = 60%, pale yellow oil; 1H -NMR (CD_3OD , 300 MHz) δ 6.94 (d, $J = 8.4$ Hz, 1H), 6.89 (t, $J = 8.4$ Hz, 1H), 6.62 (m, 1H), 6.40 (d, $J = 8.6$ Hz, 1H), 6.37 (d, $J = 7.9$ Hz, 1H), 5.65 (d, $J = 10.1$ Hz, 1H), 4.11 (m, 2H), 3.78 (s, 3H), 3.76 (s, 3H), 3.70 (s, 3H), 2.65 (t, $J = 6.8$ Hz, 2H), 2.35 (s, 6H), 1.31 (s, 6H); HRMS (FAB) calcd for $C_{25}H_{32}FN_2O_5$ $[M + H]^+$ 459.2295, found: 459.2292.

4.1.3.27. *N*-(5,6-Dimethoxypyridin-2-yl)-*N*-(2-(dimethylamino)ethyl)-5-methoxy-2,2-dimethyl-2H-chromene-6-carboxamide (**41**). Yield = 65%, pale yellow oil; 1H -NMR ($CDCl_3$, 400 MHz) δ 7.24 (m, 1H), 6.84 (m, 2H), 6.47 (m, 1H), 6.38 (d, $J = 8.3$ Hz, 1H), 5.60 (m, 1H), 4.18 (m, 2H), 3.91 (s, 3H), 3.85 (s, 3H), 3.79 (s, 3H), 2.89 (m, 2H), 2.45 (s, 6H), 1.43 (s, 6H); HRMS (FAB) calcd for $C_{24}H_{32}N_3O_5$ $[M + H]^+$ 442.2342, found 442.2350.

4.1.3.28. *N*-(5,6-Dimethoxypyridin-2-yl)-*N*-(3-(dimethylamino)propyl)-5-methoxy-2,2-dimethyl-2H-chromene-6-carboxamide (**42**). Yield = 50%, pale yellow oil; 1H -NMR (CD_3OD , 300 MHz) δ 7.04 (d, $J = 7.9$ Hz, 1H), 6.85 (d, $J = 8.2$ Hz, 1H), 6.59 (m, 1H), 6.48 (d, $J = 9.9$ Hz, 1H), 6.36 (d, $J = 8.4$ Hz, 1H), 5.70 (d, $J = 10.1$ Hz, 1H), 4.02 (m, 2H), 3.83 (s, 3H), 3.82 (s, 3H), 3.74 (s, 3H), 2.71 (m, 2H), 2.44 (s, 6H), 2.03-1.89 (m, 2H), 1.35 (s, 6H); HRMS (FAB) calcd for $C_{25}H_{34}N_3O_5$ $[M + H]^+$ 456.2498, found: 456.2495.

4.1.3.29. *N*-(2-(Diethylamino)ethyl)-*N*-(5,6-dimethoxypyridin-2-yl)-5-methoxy-2,2-dimethyl-2H-chromene-6-carboxamide (**43**). Yield = 45%, yellow oil; 1H -NMR ($CDCl_3$, 300 MHz) δ 6.97 (m,

2H), 6.49-6.38 (m, 3H), 5.70 (d, $J = 10.1$ Hz, 1H), 4.09 (m, 2H), 3.85 (s, 3H), 3.82 (s, 3H), 3.74 (s, 3H), 2.90 (m, 2H), 2.68 (m, 4H), 1.35 (s, 6H), 1.09-1.00 (m, 6H); HRMS (FAB) calcd for $C_{26}H_{36}N_3O_5$ $[M + H]^+$ 470.2655, found: 470.2649.

4.1.3.30. *N*-(2-Acetamidoethyl)-*N*-(3,4-dimethoxyphenyl)-5-methoxy-2,2-dimethyl-2H-chromene-6-carboxamide (**44**). Yield = 80%, white solid, mp = 79-80 °C; 1H -NMR ($CDCl_3$, 300 MHz) δ 6.70-6.62 (m, 4H), 6.44 (d, $J = 9.9$ Hz, 1H), 6.32 (d, $J = 8.2$ Hz, 1H), 5.61 (d, $J = 9.9$ Hz, 1H), 4.05 (t, $J = 5.3$ Hz, 2H), 3.88 (s, 3H), 3.79 (s, 3H), 3.72 (s, 3H), 3.52 (m, 2H), 2.03 (s, 3H), 1.36 (s, 6H); HRMS (FAB) calcd for $C_{25}H_{31}N_2O_6$ $[M + H]^+$ 455.2182, found: 455.2184.

4.1.3.31. *N*-(2-Acetamidoethyl)-*N*-(5,6-dimethoxypyridin-2-yl)-5-methoxy-2,2-dimethyl-2H-chromene-6-carboxamide (**45**). Yield = 45%, yellow oil; 1H -NMR ($CDCl_3$, 300 MHz) δ 6.81 (t, $J = 8.6$ Hz, 2H), 6.70 (m, 1H), 6.48 (d, $J = 9.5$ Hz, 1H), 6.43 (m, 1H), 6.37 (d, $J = 8.4$ Hz, 1H), 5.62 (d, $J = 9.9$ Hz, 1H), 4.15 (m, 2H), 3.92 (s, 3H), 3.85 (s, 3H), 3.78 (s, 3H), 3.53 (m, 2H), 1.99 (s, 3H), 1.38 (s, 6H); HRMS (FAB) calcd for $C_{24}H_{30}N_3O_6$ $[M + H]^+$ 456.2135, found 456.2135.

4.1.3.32. *N*-(3-Acetamidopropyl)-*N*-(5,6-dimethoxypyridin-2-yl)-5-methoxy-2,2-dimethyl-2H-chromene-6-carboxamide (**46**). Yield = 80%, pale yellow solid, mp = 45-46 °C; 1H -NMR ($CDCl_3$, 300 MHz) δ 6.99 (m, 1H), 6.79 (d, $J = 8.4$ Hz, 1H), 6.51 (d, $J = 10.1$ Hz, 1H), 6.44 (m, 1H), 6.35 (d, $J = 8.3$ Hz, 1H), 5.63 (d, $J = 9.9$ Hz, 1H), 4.11 (m, 2H), 3.89 (s, 3H), 3.87 (s, 3H), 3.79 (s, 3H), 3.89 (m, 2H), 2.05 (s, 3H), 1.72 (m, 2H), 1.38 (s, 6H); HRMS (FAB) calcd for $C_{25}H_{32}N_3O_6$ $[M + H]^+$ 470.2291, found: 470.2291.

4.1.3.33. *tert*-Butyl (2-(*N*-(3,4-dimethoxyphenyl)-5-methoxy-2,2-dimethyl-2H-chromene-6-carboxamido)ethyl)carbamate (**47**). Yield = 80% , white solid, mp = 70-71 °C; 1H -NMR ($CDCl_3$, 300 MHz) δ 6.73-6.63 (m, 4H), 6.45 (d, $J = 9.7$ Hz, 1H), 6.31 (d, $J = 8.4$ Hz, 1H), 5.59 (d, $J = 10.1$

Hz, 1H), 5.22 (s, 1H), 4.00 (t, $J = 5.7$ Hz, 2H), 3.89 (s, 3H), 3.78 (s, 3H), 3.70 (s, 3H), 3.41 (m, 2H), 1.44 (s, 9H), 1.36 (s, 6H); HRMS (FAB) calcd for $C_{28}H_{36}N_2O_7$ $[M]^+$ 512.2523, found: 512.2528.

4.1.3.34. *tert*-Butyl (2-(*N*-(5,6-dimethoxy-pyridin-2-yl)-5-methoxy-2,2-dimethyl-2*H*-chromene-6-carboxamido)ethyl)carbamate (48). Yield = 90% yield, pale yellow solid, mp = 64-65 °C; 1H -NMR ($CDCl_3$, 400 MHz) δ 8.09 (s, 1H), 7.74 (m, 1H), 7.32 (m, 1H), 7.14 (m, 1H), 6.75 (m, 1H), 6.46 (d, $J = 8.2$ Hz, 1H), 5.67 (m, 1H), 4.34 (m, 2H), 3.91 (s, 3H), 3.88 (s, 3H), 3.83 (s, 3H), 3.35 (m, 2H), 1.45 (s, 6H), 1.26 (s, 9H); HRMS (FAB) calcd for $C_{27}H_{36}N_3O_7$ $[M + H]^+$ 514.2553, found 514.2548.

4.1.3.35. *N*-(5,6-Dimethoxy-pyridin-2-yl)-5-methoxy-2,2-dimethyl-*N*-(2-(pyrrolidin-1-yl)ethyl)-2*H*-chromene-6-carboxamide (49). Yield = 65%, pale yellow oil; 1H -NMR ($CDCl_3$, 400 MHz) δ 6.85 (d, $J = 8.4$ Hz, 1H), 6.81 (d, $J = 8.4$ Hz, 1H), 6.45 (m, 2H), 6.40 (d, $J = 8.3$ Hz, 1H), 5.62 (d, $J = 10.0$ Hz, 1H), 4.46 (t, $J = 7.2$ Hz, 2H), 3.87 (s, 3H), 3.83 (s, 3H), 3.81 (s, 3H), 3.43 (t, $J = 7.6$ Hz, 2H), 2.14 (m, 4H), 2.00 (m, 2H), 1.93 (m, 2H), 1.38 (s, 6H); HRMS (FAB) calcd for $C_{26}H_{34}N_3O_5$ $[M + H]^+$ 468.2498, found 468.2488.

4.1.3.36. *N*-(3,4-Dimethoxyphenyl)-5-methoxy-2,2-dimethyl-*N*-(2-(piperidin-1-yl)ethyl)-2*H*-chromene-6-carboxamide (50). Yield = 70%, yellow oil; 1H -NMR ($CDCl_3$, 300 MHz) δ 6.81-6.60 (m, 4H), 6.47 (d, $J = 9.9$ Hz, 1H), 6.32 (d, $J = 8.3$ Hz, 1H), 5.58 (d, $J = 9.9$ Hz, 1H), 4.03 (t, $J = 6.8$ Hz, 2H), 3.88 (s, 3H), 3.79 (s, 3H), 3.68 (s, 3H), 2.58 (t, $J = 6.8$ Hz, 2H), 2.49 (m, 4H), 1.60 (m, 4H), 1.45 (m, 2H), 1.35 (s, 6H); HRMS (FAB) calcd for $C_{28}H_{37}N_2O_5$ $[M + H]^+$ 481.2702, found: 481.2710.

4.1.3.37. *N*-(2-Fluoro-3,4-dimethoxyphenyl)-5-methoxy-2,2-dimethyl-*N*-(2-(piperidin-1-yl)ethyl)-2*H*-chromene-6-carboxamide (51). Yield = 50%, pale yellow oil; 1H -NMR (CD_3OD , 300 MHz) δ 6.94-6.87 (m, 2H), 6.67-6.60 (m, 1H), 6.40 (d, $J = 9.8$ Hz, 1H), 6.36 (d, $J = 8.2$ Hz, 1H), 5.65 (d, $J = 10.1$ Hz, 1H), 4.22-4.10 (m, 2H), 3.79 (s, 3H), 3.76 (s, 3H), 3.70 (s, 3H), 2.65-2.51 (m, 6H), 1.63-

1.55 (m, 4H), 1.48-1.43 (m, 2H), 1.31(s, 6H); HRMS (FAB) calcd for C₂₈H₃₆FN₂O₅ [M + H]⁺ 499.2608, found: 499.2598.

4.1.3.38. *N*-(5,6-Dimethoxypyridin-2-yl)-5-methoxy-2,2-dimethyl-*N*-(2-(piperidin-1-yl)ethyl)-2H-chromene-6-carboxamide (**52**). Yield = 65%, pale yellow oil; ¹H-NMR (CDCl₃, 400 MHz) δ 7.27 (m, 1H), 6.85 (m, 2H), 6.49 (d, *J* = 10.0 Hz, 1H), 6.38 (d, *J* = 8.3 Hz, 1H), 5.60 (d, *J* = 9.6 Hz, 1H), 4.13 (m, 2H), 3.91 (s, 3H), 3.87 (s, 3H), 3.75 (s, 3H), 2.72 (m, 2H), 2.52 (m, 4H), 1.58 (m, 4H), 1.54 (m, 2H), 1.38 (s, 6H); HRMS (FAB) calcd for C₂₇H₃₆N₃O₅ [M + H]⁺ 482.2655, found 482.2648.

4.1.3.39. *N*-(5,6-Dimethoxypyridin-2-yl)-5-methoxy-2,2-dimethyl-*N*-(2-(piperidin-4-yl)ethyl)-2H-chromene-6-carboxamide (**53**). Yield = 45%, pale yellow solid, mp = 46-47 °C; ¹H-NMR (CDCl₃, 300 MHz) δ 7.03 (d, *J* = 7.1 Hz, 1H), 6.82 (d, *J* = 7.1 Hz, 1H), 6.55-6.35 (m, 3H), 5.69 (d, *J* = 10.1 Hz, 1H), 3.99 (m, 2H), 3.83 (s, 3H), 3.81 (s, 3H), 3.74 (s, 3H), 3.04 (m, 2H), 2.63-2.56 (m, 2H), 1.74 (m, 2H), 1.51 (m, 3H), 1.35 (s, 6H), 1.18 (m, 2H); HRMS (FAB) calcd for C₂₇H₃₆N₃O₅ [M + H]⁺ 482.2655, found: 482.2664.

4.1.3.40. *N*-(3,4-Dimethoxyphenyl)-5-methoxy-2,2-dimethyl-*N*-(2-morpholinoethyl)-2H-chromene-6-carboxamide (**54**). Yield = 45%, pale yellow oil; ¹H-NMR (CD₃OD, 300 MHz) δ 6.82-6.76 (m, 4H), 6.46 (d, *J* = 9.7 Hz, 1H), 6.32 (d, *J* = 8.3 Hz, 1H), 5.68 (d, *J* = 10.1 Hz, 1H), 4.04 (t, *J* = 6.8 Hz, 2H), 3.85 (s, 3H), 3.72 (s, 3H), 3.68 (m, 4H), 3.59 (s, 3H), 2.57 (t, *J* = 6.6 Hz, 2H), 2.50 (m, 4H), 1.32 (s, 6H); HRMS (FAB) calcd for C₂₇H₃₅N₂O₆ [M + H]⁺ 483.2495, found: 483.2500.

4.1.3.41. *N*-(2-Fluoro-3,4-dimethoxyphenyl)-5-methoxy-2,2-dimethyl-*N*-(2-morpholinoethyl)-2H-chromene-6-carboxamide (**55**). Yield = 50%, pale yellow oil, mp = 55-59 °C; ¹H-NMR (CD₃OD, 300 MHz) δ 6.95-6.90 (m, 2H), 6.66-6.60 (m, 1H), 6.41 (d, *J* = 10.1 Hz, 1H), 6.37 (d, *J* = 8.4 Hz, 1H), 5.66 (d, *J* = 9.9 Hz, 1H), 4.25-4.15 (m, 2H), 3.80 (s, 3H), 3.76 (s, 3H), 3.70 (s, 3H), 3.65 (m,

4H), 2.60-2.40 (m, 6H), 1.31 (s, 6H); HRMS (FAB) calcd for C₂₇H₃₄FN₂O₆ [M + H]⁺ 501.2401, found: 501.2408.

4.1.3.42. *N*-(5,6-Dimethoxy-pyridin-2-yl)-5-methoxy-2,2-dimethyl-*N*-(2-morpholinoethyl)-2*H*-chromene-6-carboxamide (**56**). Yield = 65%, pale yellow oil, mp = 45-46 °C; ¹H-NMR (CDCl₃, 400 MHz) δ 7.27 (m, 1H), 6.84 (m, 2H), 6.49 (d, *J* = 10.0 Hz, 1H), 6.38 (d, *J* = 8.3 Hz, 1H), 5.61 (d, *J* = 10.0 Hz, 1H), 4.12 (m, 2H), 3.91 (s, 3H), 3.87 (s, 3H), 3.75 (s, 3H), 3.67 (m, 2H), 2.59 (m, 4H), 1.65 (m, 4H), 1.38 (s, 6H); HRMS (FAB) calcd for C₂₆H₃₄N₃O₆ [M + H]⁺ 484.2448, found 484.2442.

4.1.3.43. *N*-(3,4-Dimethoxyphenyl)-5-methoxy-2,2-dimethyl-*N*-(2-(piperazin-1-yl)ethyl)-2*H*-chromene-6-carboxamide (**57**). Yield = 50%, pale yellow solid, mp = 90-91 °C; ¹H-NMR (CD₃OD, 300 MHz) δ 6.82-6.76 (m, 4H), 6.45 (d, *J* = 10.1 Hz, 1H), 6.32 (d, *J* = 8.3 Hz, 1H), 5.67 (d, *J* = 9.9 Hz, 1H), 4.10-4.04 (m, 2H), 3.85-3.64 (m, 4H), 3.84 (s, 3H), 3.72 (s, 3H), 3.66 (s, 3H), 2.60-2.40 (m, 6H), 1.32 (s, 6H); HRMS (FAB) calcd for C₂₇H₃₆N₃O₅ [M + H]⁺ 482.2655, found: 482.2655.

4.1.3.44. *N*-(2-Fluoro-3,4-dimethoxyphenyl)-5-methoxy-2,2-dimethyl-*N*-(2-(piperazin-1-yl)ethyl)-2*H*-chromene-6-carboxamide (**58**). Yield = 50%, pale yellow solid, mp = 88-89 °C; ¹H-NMR (CD₃OD, 300 MHz) δ 6.94-6.89 (m, 2H), 6.64-6.61 (m, 1H), 6.40 (d, *J* = 10.4 Hz, 1H), 6.37 (d, *J* = 9.5 Hz, 1H), 5.65 (d, *J* = 9.9 Hz, 1H), 4.18-4.11 (m, 2H), 3.80-3.68 (m, 4H), 3.79 (s, 3H), 3.76 (s, 3H), 3.70 (s, 3H), 2.60-2.22 (m, 6H), 1.31 (s, 6H); HRMS (FAB) calcd for C₂₇H₃₅FN₃O₅ [M + H]⁺ 500.2561, found: 500.2561.

4.1.3.45. *N*-(5,6-Dimethoxy-pyridin-2-yl)-5-methoxy-2,2-dimethyl-*N*-(2-(piperazin-1-yl)ethyl)-2*H*-chromene-6-carboxamide (**59**). Yield = 60%, pale yellow solid, mp = 53-54 °C; ¹H-NMR (CD₃OD, 300 MHz) δ 7.03 (d, *J* = 7.9 Hz, 1H), 6.87 (d, *J* = 8.0 Hz, 1H), 6.56 (m, 1H), 6.50 (d, *J* = 9.9 Hz, 1H), 6.37 (d, *J* = 8.2 Hz, 1H), 5.69 (d, *J* = 9.9 Hz, 1H), 4.11 (m, 2H), 3.83 (s, 6H), 3.74 (s, 3H), 2.81 (m,

4H), 2.66 (m, 2H), 2.51 (m, 4H), 1.35 (s, 6H); HRMS (FAB) calcd for C₂₆H₃₅N₄O₅ [M + H]⁺ 483.2607, found: 483.2604.

4.1.3.46. *N*-(3,4-Dimethoxyphenyl)-5-methoxy-2,2-dimethyl-*N*-(2-(4-methylpiperazin-1-yl)ethyl)-2*H*-chromene-6-carboxamide (60). Yield = 50%, pale yellow solid, mp = 72-73 °C; ¹H-NMR (CD₃OD, 300 MHz) δ 6.81-6.75 (m, 4H), 6.45 (d, *J* = 9.9 Hz, 1H), 6.32 (d, *J* = 8.4 Hz, 1H), 5.67 (d, *J* = 10.1 Hz, 1H), 4.03 (t, *J* = 6.8 Hz, 2H), 3.85 (s, 3H), 3.72 (s, 3H), 3.66 (s, 3H), 2.62-2.42 (m, 6H), 2.36 (m, 4H), 1.32 (s, 6H), 1.28 (s, 3H); HRMS (FAB) calcd for C₂₈H₃₈N₃O₅ [M + H]⁺ 496.2811, found: 496.2808.

4.1.3.47. *N*-(2-Fluoro-3,4-dimethoxyphenyl)-5-methoxy-2,2-dimethyl-*N*-(2-(4-methylpiperazin-1-yl)ethyl)-2*H*-chromene-6-carboxamide (61). Yield = 50%, pale yellow oil; ¹H-NMR (CD₃OD, 300 MHz) δ 6.94-6.88 (m, 2H), 6.67-6.60 (m, 1H), 6.41 (d, *J* = 10.6 Hz, 1H), 6.36 (d, *J* = 8.6 Hz, 1H), 5.65 (d, *J* = 9.9 Hz, 1H), 4.23-4.13 (m, 2H), 3.80 (s, 3H), 3.74 (s, 3H), 3.70 (s, 3H), 2.62-2.41 (m, 10H), 2.32 (s, 3H), 1.31 (s, 6H); HRMS (FAB) calcd for C₂₈H₃₇FN₃O₅ [M + H]⁺ 514.2717, found: 514.2709.

4.1.3.48. *N*-(5,6-Dimethoxypyridin-2-yl)-5-methoxy-2,2-dimethyl-*N*-(2-(4-methylpiperazin-1-yl)ethyl)-2*H*-chromene-6-carboxamide (62). Yield = 40%, pale yellow solid, mp = 45-46 °C; ¹H-NMR (CD₃OD, 300 MHz) δ 6.87-6.79 (m, 2H), 6.50 (d, *J* = 9.9 Hz, 1H), 6.49-6.39 (m, 1H), 6.37 (d, *J* = 8.0 Hz, 1H), 5.61 (d, *J* = 9.9 Hz, 1H), 4.08 (m, 2H), 3.90 (s, 3H), 3.87 (s, 3H), 3.79 (s, 3H), 2.70 (t, *J* = 6.8 Hz, 2H), 2.65-2.33 (m, 8H), 2.30 (s, 3H), 1.38 (s, 6H); HRMS (FAB) calcd for C₂₇H₃₇N₄O₅ [M + H]⁺ 497.2764, found: 497.2763.

4.1.3.49. 6-((3,4-Dimethoxybenzyl)thio)-5-methoxy-2,2-dimethyl-2*H*-chromene (63). Yield = 65%, pale yellow solid, mp = 70-73 °C; ¹H-NMR (CD₃OD, 300 MHz) δ 7.30-7.17 (m, 6H), 6.93 (dd, *J* =

8.2, 1.3 Hz, 1H), 6.57 (t, $J = 9.0$ Hz, 1H), 6.48-6.35 (m, 3H), 5.65 (d, $J = 9.9$ Hz, 1H), 5.38 (d, $J = 14.3$ Hz, 1H), 4.61 (d, $J = 14.1$ Hz, 1H), 3.81 (s, 3H), 3.70 (s, 3H), 3.65 (s, 3H), 1.30 (s, 6H); HRMS (FAB) calcd for $C_{28}H_{29}NO_5$ $[M + H]^+$ 460.2046, found: 460.2035.

4.1.3.50. *N-Benzyl-N-(2-fluoro-3,4-dimethoxyphenyl)-5-methoxy-2,2-dimethyl-2H-chromene-6-carboxamide (64)*. Yield = 60%, pale yellow solid, mp = 76-77 °C; 1H -NMR (CD_3OD , 300 MHz) δ 7.30-7.17 (m, 5H), 6.93 (dd, $J = 8.2, 1.3$ Hz, 1H), 6.57 (t, $J = 9.0$ Hz, 1H), 6.48-6.35 (m, 3H), 5.65 (d, $J = 9.9$ Hz, 1H), 5.38 (d, $J = 14.3$ Hz, 1H), 4.61 (d, $J = 14.1$ Hz, 1H), 3.81 (s, 3H), 3.70 (s, 3H), 3.65 (s, 3H), 1.30 (s, 6H); HRMS (FAB) calcd for $C_{28}H_{29}FNO_5$ $[M + H]^+$ 478.2030, found: 478.2036.

4.1.3.51. *N-Benzyl-N-(5,6-dimethoxypyridin-2-yl)-5-methoxy-2,2-dimethyl-2H-chromene-6-carboxamide (65)*. Yield = 70%, pale yellow solid, mp = 71-72 °C; 1H -NMR ($CDCl_3$, 400 MHz) δ 7.40 (m, 2H), 7.22 (m, 4H), 6.88 (m, 1H), 6.70 (m, 1H), 6.50 (m, 1H), 6.47 (m, 1H), 5.62 (m, 1H), 5.19 (s, 2H), 3.91 (s, 3H), 3.88 (s, 3H), 3.75 (s, 3H), 1.45 (s, 6H); HRMS (FAB) calcd for $C_{27}H_{29}N_2O_5$ $[M + H]^+$ 461.2076, found 461.2079.

4.1.3.52. *N-(5,6-Dimethoxypyridin-2-yl)-N-(4-fluorobenzyl)-5-methoxy-2,2-dimethyl-2H-chromene-6-carboxamide (66)*. Yield = 86%, white solid, mp = 45-46 °C; 1H -NMR ($CDCl_3$, 300 MHz) δ 7.34 (m, 1H), 6.96 (d, $J = 8.6$ Hz, 1H), 6.93 (d, $J = 8.7$ Hz, 1H), 6.86 (d, $J = 8.2$ Hz, 1H), 6.71 (d, $J = 7.5$ Hz, 1H), 6.49 (d, $J = 10.0$ Hz, 1H), 6.37 (d, $J = 8.6$ Hz, 1H), 6.40-6.15 (m, 1H), 5.61 (d, $J = 10.0$ Hz, 1H), 5.15 (s, 1H), 3.89 (s, 3H), 3.85 (s, 3H), 3.75 (s, 3H), 1.38 (s, 6H); HRMS (FAB) calcd for $C_{27}H_{28}FN_2O_5$ $[M + H]^+$ 479.1982, found 479.1982.

4.1.3.53. *N-(4-Chlorobenzyl)-N-(5,6-dimethoxypyridin-2-yl)-5-methoxy-2,2-dimethyl-2H-chromene-6-carboxamide (67)*. Yield = 86%, white solid, mp = 45-46 °C; 1H -NMR ($CDCl_3$, 300 MHz) δ 7.32 (m, 2H), 7.26-7.20 (m, 2H), 6.86 (d, $J = 8.2$ Hz, 1H), 6.72 (d, $J = 8.0$ Hz, 1H), 6.50 (d,

$J = 10.0$ Hz, 1H), 6.37 (d, $J = 8.2$ Hz, 1H), 6.37-6.22 (m, 1H), 5.61 (d, $J = 9.9$ Hz, 1H), 5.15 (s, 2H), 3.89 (s, 3H), 3.85 (s, 3H), 3.75 (s, 3H), 1.38 (s, 6H); HRMS (FAB) calcd for $C_{27}H_{28}ClN_2O_5$ $[M + H]^+$ 495.1687, found 495.1687.

4.1.3.54. *N*-(5,6-Dimethoxypyridin-2-yl)-5-methoxy-*N*-(4-methoxybenzyl)-2,2-dimethyl-2H-chromene-6-carboxamide (68). Yield = 89%, white solid, mp = 44-45 °C; 1H -NMR ($CDCl_3$, 300 MHz) δ 7.35-7.25 (m, 2H), 6.87 (d, $J = 8.4$ Hz, 1H), 6.79 (m, 2H), 6.71 (d, $J = 7.1$ Hz, 1H), 6.50 (d, $J = 10.0$ Hz, 1H), 6.36 (d, $J = 8.4$ Hz, 1H), 6.36-6.25 (m, 1H), 5.60 (d, $J = 9.8$ Hz, 1H), 5.13 (s, 2H), 3.90 (s, 3H), 3.86 (s, 3H), 3.76 (s, 3H), 3.74 (s, 3H), 1.37 (s, 6H); HRMS (FAB) calcd for $C_{28}H_{31}N_2O_6$ $[M + H]^+$ 491.2182, found 491.2182.

4.1.3.55. *N*-(5,6-Dimethoxypyridin-2-yl)-5-methoxy-2,2-dimethyl-*N*-(4-methylbenzyl)-2H-chromene-6-carboxamide (69). Yield = 83%, white solid, mp = 44-45 °C; 1H -NMR (CD_3OD , 300 MHz) δ 7.22 (m, 2H), 7.07 (m, 2H), 6.91 (d, $J = 10.5$ Hz, 1H), 6.88 (d, $J = 8.4$ Hz, 1H), 6.48 (d, $J = 9.9$ Hz, 1H), 6.36 (d, $J = 8.7$ Hz, 1H), 5.68 (d, $J = 10.0$ Hz, 1H), 5.12 (s, 2H), 3.82 (s, 3H), 3.79 (s, 3H), 3.69 (s, 3H), 2.27 (s, 3H), 1.34 (s, 6H); HRMS (FAB) calcd for $C_{28}H_{31}N_2O_5$ $[M + H]^+$ 475.2233, found 475.2233.

4.1.3.56. *N*-(5,6-Dimethoxypyridin-2-yl)-*N*-(3-fluorobenzyl)-5-methoxy-2,2-dimethyl-2H-chromene-6-carboxamide (70). Yield = 83%, white solid, mp = 43-44 °C; 1H -NMR ($CDCl_3$, 300 MHz) δ 7.20 (m, 3H), 6.89 (m, 2H), 6.73 (d, $J = 8.0$ Hz, 1H), 6.50 (d, $J = 10.0$ Hz, 1H), 6.38 (d, 1H, $J = 8.4$ Hz), 6.39-6.15 (m, 1H), 5.61 (d, $J = 9.9$ Hz, 1H), 5.18 (s, 2H), 3.88 (s, 3H), 3.86 (s, 3H), 3.75 (s, 3H), 1.38 (s, 6H); HRMS (FAB) calcd for $C_{27}H_{28}FN_2O_5$ $[M + H]^+$ 479.1982, found 479.1982.

4.1.3.57. *N*-(3-Chlorobenzyl)-*N*-(5,6-dimethoxypyridin-2-yl)-5-methoxy-2,2-dimethyl-2H-chromene-6-carboxamide (71). Yield = 89% yield, white solid, mp = 44-45 °C; 1H -NMR ($CDCl_3$,

300 MHz) δ 7.49 (s, 1H), 7.21 (m, 3H), 6.87 (d, $J = 8.4$ Hz, 1H), 6.73 (d, $J = 8.0$ Hz, 1H), 6.50 (d, $J = 10.0$ Hz, 1H), 6.39 (d, $J = 8.4$ Hz, 1H), 6.41-6.30 (m, 1H), 5.62 (d, $J = 9.9$ Hz, 1H), 5.15 (s, 2H), 3.89 (s, 3H), 3.85 (s, 3H), 3.75 (s, 3H), 1.38 (s, 6H); HRMS (FAB) calcd for $C_{27}H_{28}ClN_2O_5$ $[M + H]^+$ 495.1687, found 495.1687.

4.1.3.58. *N-(5,6-Dimethoxypyridin-2-yl)-5-methoxy-2,2-dimethyl-N-(pyridin-2-ylmethyl)-2H-chromene-6-carboxamide (72)*. Yield = 65% yield, pale yellow oil; 1H -NMR ($CDCl_3$, 400 MHz) δ 8.61 (m, 1H), 7.64 (m, 1H), 7.52 (m, 1H), 7.27 (m, 1H), 7.14 (m, 1H), 6.91 (d, $J = 8.4$ Hz, 1H), 6.79 (m, 1H), 6.52 (d, $J = 9.6$ Hz, 1H), 6.39 (d, $J = 8.4$ Hz, 1H), 5.62 (d, $J = 10.0$ Hz, 1H), 5.33 (s, 2H), 3.87 (s, 3H), 3.76 (s, 3H), 3.75 (s, 3H), 1.39 (s, 6H); HRMS (FAB) calcd for $C_{26}H_{28}N_3O_5$ $[M + H]^+$ 462.2029, found 462.2037.

4.1.3.59. *N-(5,6-Dimethoxypyridin-2-yl)-5-methoxy-2,2-dimethyl-N-(pyridin-3-ylmethyl)-2H-chromene-6-carboxamide (73)*. Yield = 65%, pale yellow oil; 1H -NMR ($CDCl_3$, 400 MHz) δ 8.62 (d, 1H), 8.47 (d, $J = 4.0$ Hz, 1H), 7.80 (d, $J = 7.6$ Hz, 1H), 7.26 (m, 2H), 6.87 (d, $J = 8.4$ Hz, 1H), 6.72 (d, $J = 7.6$ Hz, 1H), 6.52 (d, $J = 10.0$ Hz, 1H), 6.41 (d, $J = 8.3$ Hz, 1H), 5.61 (d, $J = 10.0$ Hz, 1H), 5.22 (s, 2H), 3.90 (s, 3H), 3.83 (s, 3H), 3.76 (s, 3H), 1.38 (s, 6H); HRMS (FAB) calcd for $C_{26}H_{28}N_3O_5$ $[M + H]^+$ 462.2029, found 462.2032.

4.1.3.60. *N-(5,6-Dimethoxypyridin-2-yl)-5-methoxy-2,2-dimethyl-N-(pyridin-4-ylmethyl)-2H-chromene-6-carboxamide (74)*. Yield = 65%, pale yellow oil; 1H -NMR ($CDCl_3$, 400 MHz) δ 8.62 (m, 1H), 7.78 (m, 1H), 7.27 (m, 1H), 7.24 (m, 1H), 6.87 (d, $J = 8.4$ Hz, 1H), 6.71 (d, $J = 8.2$ Hz, 1H), 6.48 (m, 2H), 5.61 (m, 2H), 5.20 (s, 2H), 3.90 (s, 3H), 3.83 (s, 3H), 3.76 (s, 3H), 1.38 (s, 6H); HRMS (FAB) calcd for $C_{26}H_{28}N_3O_5$ $[M + H]^+$ 462.2029, found 462.2037.

4.1.3.61. *N-(3,4-Dimethoxyphenyl)-5-methoxy-2,2-dimethyl-N-phenyl-2H-chromene-6-*

carboxamide (75). Yield = 40%, pale yellow solid, mp = 66-67 °C; ¹H-NMR (CDCl₃, 300 MHz) δ 7.26-7.15 (m, 5H), 6.94 (d, *J* = 8.3 Hz, 1H), 6.72 (m, 3H), 6.48 (d, *J* = 10.1 Hz, 1H), 6.38 (d, *J* = 8.4 Hz, 1H), 5.58 (d, *J* = 9.9 Hz, 1H), 3.93 (s, 3H), 3.82 (s, 3H), 3.74 (s, 3H), 1.37 (s, 6H); HRMS (FAB) calcd for C₂₇H₂₈NO₅ [M + H]⁺ 446.1967, found: 446.1965.

4.1.3.62. *N*-(3,4-Dimethoxyphenyl)-*N*-(4-fluorophenyl)-5-methoxy-2,2-dimethyl-2H-chromene-6-carboxamide (76). Yield = 40%, pale yellow solid, mp = 60-61 °C; ¹H-NMR (CDCl₃, 300 MHz) δ 7.83-7.76 (m, 1H), 7.61-7.48 (m, 2H), 7.23-7.13 (m, 1H), 6.95 (m, 1H), 6.91 (d, *J* = 8.4 Hz, 1H), 6.71 (m, 2H), 6.48 (d, *J* = 10.1 Hz, 1H), 6.40 (d, *J* = 8.4 Hz, 1H), 5.61 (d, *J* = 9.9 Hz, 1H), 3.92 (s, 3H), 3.82 (s, 3H), 3.74 (s, 3H), 1.38 (s, 6H); HRMS (FAB) calcd for C₂₇H₂₇FNO₅ [M + H]⁺ 464.1873, found: 464.1879.

4.1.3.63. *N*-(4-Chlorophenyl)-*N*-(3,4-dimethoxyphenyl)-5-methoxy-2,2-dimethyl-2H-chromene-6-carboxamide (77). Yield = 40%, pale yellow solid, mp = 71-72 °C; ¹H-NMR (CDCl₃, 300 MHz) δ 7.21-7.15 (m, 4H), 6.89 (d, *J* = 8.4 Hz, 1H), 6.68 (m, 3H), 6.45 (d, *J* = 9.9 Hz, 1H), 6.37 (d, *J* = 8.7 Hz, 1H), 5.60 (d, *J* = 9.9 Hz, 1H), 3.89 (s, 3H), 3.78 (s, 3H), 3.71 (s, 3H), 1.35 (s, 6H); HRMS (FAB) calcd for C₂₇H₂₇ClNO₅ [M + H]⁺ 480.1578, found: 480.1574.

4.1.3.64. *N*-(3,4-Dimethoxyphenyl)-5-methoxy-*N*-(4-methoxyphenyl)-2,2-dimethyl-2H-chromene-6-carboxamide (78). Yield = 40%, pale yellow solid, mp = 70-71 °C; ¹H-NMR (CDCl₃, 300 MHz) δ 7.21-7.13 (m, 2H), 6.92 (d, *J* = 8.4 Hz, 1H), 6.88-6.58 (m, 5H), 6.47 (d, *J* = 9.9 Hz, 1H), 6.38 (dd, *J* = 8.4, 0.6 Hz, 1H), 5.58 (d, *J* = 10.2 Hz, 1H), 3.90 (s, 3H), 3.82 (s, 3H), 3.73 (s, 3H), 1.35 (s, 6H); HRMS (FAB) calcd for C₂₈H₃₀NO₆ [M + H]⁺ 476.2073, found: 476.2077.

4.1.3.65. *N*-(3,4-Dimethoxyphenyl)-5-methoxy-2,2-dimethyl-*N*-(*p*-tolyl)-2H-chromene-6-carboxamide (79). Yield = 40%, pale yellow solid, mp = 62-63 °C; ¹H-NMR (CDCl₃, 300 MHz) δ

7.83-7.77 (m, 1H), 7.57-7.50 (m, 1H), 7.22-7.00 (m, 2H), 6.92 (d, $J = 8.4$ Hz, 1H), 6.71 (m, 3H), 6.50 (d, $J = 9.9$ Hz, 1H), 6.39 (d, $J = 8.2$ Hz, 1H), 5.61 (d, $J = 9.9$ Hz, 1H), 3.93 (s, 3H), 3.80 (s, 3H), 3.74 (s, 3H), 2.29 (s, 3H), 1.37 (s, 6H); HRMS (FAB) calcd for $C_{28}H_{30}NO_5$ $[M + H]^+$ 460.2124, found: 460.2126.

4.2. Molecular modeling

All performances of computational works were carried out on the Tripos Sybyl-X 2.1³³ (Tripos Inc, St Louis, MO, USA) molecular modeling package. The ligands were prepared as Mol2 format using sketch modules embedded in Sybyl. Gasteiger-Hückel charges were assigned to all ligand's atoms. Each ligand was energy-minimized using a standard Tripos force field with convergence to maximum derivatives of $0.001 \text{ kcal mol}^{-1} \cdot \text{Å}^{-1}$. For docking modeling, we used the homology model of full-length of human Hsp90 α dimer in an open conformation, which was prepared previously.^{29,30} The compound L130 was docked into the active site of hHsp90 homology model structure using Surflex-Dock algorithm. The active site was defined by generating a protomol based on the ATP binding pocket of the C-terminal domain. The protomol was built in the active site from the hydrogen-containing protein mol2 file using optimized parameters (threshold factor of 0.4 Å and bloat of 1 Å). Docking was performed with default parameters and 20 maximum conformation numbers. Binding affinity of each docking pose of ligand was calculated by Surflex-Dock score ($-\log K_d$).

4.3. Materials and Methods

4.3.1. Reagents and antibodies

Phosphatase inhibitor and protease inhibitor cocktail tablets were purchased from Roche Applied Sciences (Penzberg, GER). The antibodies that were used include: STAT3 (Abcam, Cambridge, MA); anti-AKT, phospho-AKT (Ser473), ERK, phospho-ERK (Thr202/Tyr204), phospho-STAT3 (Tyr705) (Cell Signaling, Beverly, CA); MEK, phospho-MEK (Ser218/222) (Santa Cruz Biotechnology, Santa Cruz, CA); β -actin (Sigma-Aldrich, Saint Louis, MO). The secondary antibodies were horseradish

peroxidase (HRP)-conjugated anti-rabbit and mouse IgG (Bio-Rad Laboratories, Hercules, CA).

4.3.2. Breast cancer cell culture

The TNBC cell lines MDA-MB-231 (PerkinElmer, Inc. CT) and 4T1 (Japanese Collection of Research Bioresources Cell Bank) were cultured in MEM or RPMI 1640 (Gibco, MD) containing 10% fetal bovine serum (FBS), streptomycin-penicillin (100 U/ml) and Fungizone (0.625 µg/ml). Cells were incubated at 37 °C in an atmosphere of 5% CO₂.

4.3.3. Cell viability assay

Cell viability was measured using the CellTiter 96* Aqueous One Solution Cell Proliferation Assay [MTS, 3-(4,5-dimethylthiazol-2-yl)-5-(3-carboxymethoxyphenyl)-2-(4-sulfophenyl)-2H-tetrazolium] (Promega, WI, USA), according to the manufacturer's instructions. The quantity of formazan product was determined by measuring absorbance at 490 nm using a Spectramax Plus384 microplate analyzer (Molecular Devices, Sunnyvale, CA, USA).

4.3.4. Western blot analysis

Cells were solubilized in lysis buffer [30 mM NaCl, 0.5% Triton X-100, 50 mM Tris-HCl (pH 7.4)] containing phosphatase and protease inhibitor cocktail tablets. Supernatant was collected after centrifugation (14,000 g, 4°C, 20 min) and protein concentrations were measured with a Bradford protein assay kit (Bio-Rad Laboratories). Equal quantities of protein (30 µg) were subjected to SDS-PAGE and electrotransferred onto a nitrocellulose membrane (GE Healthcare Life Sciences, Buckinghamshire, UK). The membranes were incubated overnight at 4°C with primary antibodies diluted in 5% BSA [AKT (1:2000), phospho-AKT (1:2000), ERK (1:2000), phospho-ERK (1:2000), , STAT3 (1:3000), phospho-STAT3 (1:2000), MEK (1:3000), phospho-MEK (1:3000) or β-actin (1:5000)] and membrane were incubated with HRP-conjugated rabbit or mouse secondary antibody (1:3000–1:10,000). Signal intensity was detected using a

Chemiluminescence Kit (Thermo Fisher Scientific Fremont, CA) on X-ray film (Agfa Healthcare, Mortsel, Belgium) and quantitated using AlphaEaseFC software (Alpha Innotech, San Leandro, CA).

4.3.5. Statistical analysis

All data were analyzed using GraphPad Prism 5.0 statistical software (San Diego, CA). The results are presented as mean \pm SEM of at least three independent experiments. Data were analyzed by one-way ANOVA. Significance between multiple experimental groups was determined using the Bonferroni post hoc test and defined at $p^* < 0.05$.

Acknowledgments

This work was supported by a grant (HI12C1852, 1720340) from the Korea Health Technology R&D Project through the Korea Health Industry Development Institute (KHIDI), funded by the Ministry of Health & Welfare, Republic of Korea.

References and notes

1. Trepel J, Mollapour M, Giaccone G, Neckers L, Laplante M, Sabatini DM. mTOR signaling in growth control and disease. *Cell*. 2012;149:274-293.
2. Whitesell L, Lindquist SL. HSP90 and the chaperoning of cancer. *Nat Rev Cancer*. 2005;5:761-772.
3. Hanahan D, Weinberg RA. Hallmarks of cancer. *Cell*. 2000;100:57-70.
4. Sawai A, Chandarlapaty S, Greulich H, Gonen M, Ye Q, Arteaga CL, Sellers W, Rosen N, Solit DB. Inhibition of Hsp90 down-regulates mutant epidermal growth factor receptor (EGFR) expression and sensitizes EGFR mutant tumors to paclitaxel. *Cancer Res*. 2008;68:589-596.
5. Bao R, Lai CJ, Wang DG, Qu H, Yin L, Zifcak B, Tao X, Wang L, Atoyian R, Samson M, Forrester J, Xu G-X, DellaRocca S, Borek M, Zhai H-X, Cai X, Qian C. Targeting heat shock protein 90 with CUDC-305 overcomes erlotinib resistance in non-small cell lung cancer. *Mol Cancer Ther*.

2009;8:3296-3306.

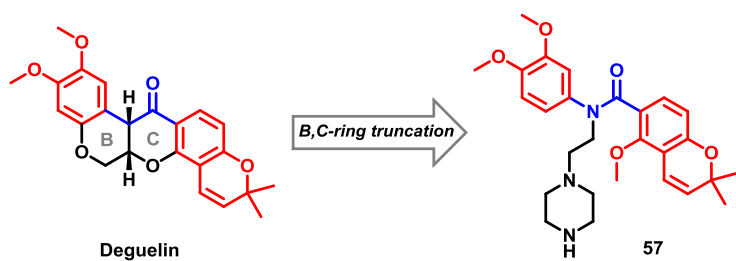
6. Wainberg ZA, Anghel A, Rogers AM, Desai AJ, Kalous D, Conklin D, Ayala R, O'Brien NA, Quadt C, Akimov M, Slamon DJ, Finn RS. Inhibition of HSP90 with AUY922 induces synergy in HER2-amplified trastuzumab-resistant breast and gastric cancer. *Mol Cancer Ther.* 2013;12:509-519.
7. Bhat R, Tummalapalli SR, Rotella DP. Progress in the discovery and development of heat shock protein 90 (Hsp90) inhibitors. *J Med Chem.* 2014;57:8718-8728.
8. Wang M, Shen A, Zhang C, Song Z, Ai J, Liu H, Sun L, Ding J, Geng M, Zhang A. Development of heat shock protein (HSP90) inhibitors to combat resistance to tyrosine kinase inhibitors through Hsp90-kinase interactions. *J Med Chem.* 2016;59:5563-5586.
9. Young JC, Agashe VR, Siegers K, Hartl FU. Pathways of chaperone-mediated protein folding in the cytosol. *Nat Rev Mol Cell Biol.* 2004;5:781-791.
10. Neckers L, Workman P. Hsp90 molecular chaperone inhibitors: are we there yet? *Clin Cancer Res.* 2012;18:64-76.
11. Whitesell L, Lindquist SL. HSP90 and the chaperoning of cancer. *Nat Rev Cancer.* 2005;5:761-772.
12. Bagatell R, Whitesell L. Altered Hsp90 function in cancer: a unique therapeutic opportunity. *Mol Cancer Ther.* 2004;3:1021-1030.
13. Eskew JD, Sadikot T, Morales P, Duren A, Dunwiddie I, Swink M, Zhang X, Hembruff S, Donnelly A, Rajewski RA, Blagg BSJ, Manjarrez JR, Matts RL, Holzbeierlein JM, Vielhauer GA. Development and characterization of a novel C-terminal inhibitor of Hsp90 in androgen dependent and independent prostate cancer cells. *BMC Cancer.* 2011;11:468.
14. Ke Q, Costa M. Hypoxia-inducible factor-1 (HIF-1). *Mol Pharm.* 2006;70:1469-1480.
15. Koh MY, Spivak-Kroizman TR, Powis G. HIF-1 regulation: not so easy come, easy go. *Trends Biochem Sci.* 2008;33:526-534.
16. Semenza GL. Targeting HIF-1 for cancer therapy. *Nat Rev Cancer.* 2003;3:721-732.

17. Xia Y, Choi HK, Lee K. Recent advances in hypoxia-inducible factor (HIF)-1 inhibitors. *Eur J Med Chem.* 2012;49:24-40.
18. Kalimutho M, Parsons K, Mittal D, Lopez JA, Srihari S, Khanna KK. Targeted Therapies for Triple-Negative Breast Cancer: Combating a Stubborn Disease. *Trends Pharmacol Sci.* 2015;36:822-846.
19. Cheng Q, Chang JT, Geradts J, Neckers LM, Haystead T, Spector NL, Lyerly HK. Amplification and high-level expression of heat shock protein 90 marks aggressive phenotypes of human epidermal growth factor receptor 2 negative breast cancer. *Breast Cancer Res.* 2012;14:R62.
20. Neckers L, Workman P. Hsp90 molecular chaperone inhibitors: are we there yet?. *Clin Cancer Res.* 2012;18:64-76.
21. Bohonowych JE, Gopal U, Isaacs JS. Hsp90 as a gatekeeper of tumor angiogenesis: clinical promise and potential pitfalls. *J Oncol.* 2010;2010:412985.
22. Solarova Z, Mojzis J, Solar P. Hsp90 inhibitor as a sensitizer of cancer cells to different therapies (review). *Int J Oncol.* 2015;46:907-926.
23. Tsutsumi S, Beebe K, Neckers L. Impact of heat-shock protein 90 on cancer metastasis. *Future Oncol.* 2009;5:679-688.
24. Isaacs JS, Xu W, Neckers L. Heat shock protein 90 as a molecular target for cancer therapeutics. *Cancer Cell.* 2003;3:213-217.
25. Bocchini CE, Kasembeli MM, Roh SH, Tweardy DJ. Contribution of chaperones to STAT pathway signaling. *JAKSTAT.* 2014;3:e970459.
26. Chatterjee M, Jain S, Stuhmer T, Andrulis M, Ungethum U, Kuban RJ, Lorentz H, Bommert K, Topp M, Kramer D, Muller-Hermelink HK, Einsele H, Greiner A, Bargou RC. STAT3 and MAPK signaling maintain overexpression of heat shock proteins 90alpha and beta in multiple myeloma cells, which critically contribute to tumor-cell survival. *Blood.* 2007;109:720-728.
27. (a) Lee HY. Molecular mechanisms of deguelin-induced apoptosis in transformed human bronchial epithelial cells. *Biochem Pharmacol.* 2004;68:1119-1124. (b) Udeani GO, Gerhauser C, Thomas CF,

- Moon RC, Kosmeder JW, Kinghorn AD, Moriarty RM, Pezzuto JM. Cancer chemopreventive activity mediated by deguelin, a naturally occurring rotenoid. *Cancer Res.* 1997;57:3424-3428. (c) Udeani GO, Zhao GM, Shin YG, Kosmeder JW, Beecher CW, Kinghorn AD, Moriarty RM, Moon RC, Pezzuto JM. Pharmacokinetics of deguelin, a cancer chemopreventive agent in rats. *Cancer Chemother Pharmacol.* 2001;47:263-268. (d) Oh SH, Woo JK, Yazici YD, Myers JN, Kim WY, Jin Q, Hong SS, Park HJ, Suh YG, Kim KW. Structural basis for depletion of heat shock protein 90 client proteins by deguelin. *J Natl Cancer Inst.* 2007;99:949-961.
28. Chang D-J, An H, Kim K-S, Kim HH, Jung J, Lee JM, Kim N-J, Han YT, Yun H, Lee S, Lee G, Lee S, Lee JS, Cha J-H, Park J-H, Park JW, Lee S-C, Kim SG, Kim JH, Lee H-Y, Kim K-W, Suh Y-G. Design, synthesis, and biological evaluation of novel deguelin-based heat shock protein 90 (HSP90) inhibitors targeting proliferation and angiogenesis. *J Med Chem.* 2012;55:10863-10884.
29. Lee S-C, Min H-Y, Choi H, Bae SY, Park KH, Hyun SY, Lee HJ, Moon J, Park S-H, Kim JY, An H, Park S-J, Seo JH, Lee S, Kim Y-M, Park H-J, Lee SK, Lee J, Lee J, Kim K-W, Suh Y-G, Lee H-Y. Deguelin analogue SH-1242 inhibits Hsp90 activity and exerts potent anticancer efficacy with limited neurotoxicity. *Cancer Res.* 2016;76:686-699.
30. Kim HS, Hong M, Lee S-C, Lee H-Y, Suh Y-G, Oh D-C, Seo JH, Choi H, Kim JY, Kim K-W, Kim JH, Kim J, Kim Y-M, Park S-J, Park H-J, Lee J. Ring-truncated deguelin derivatives as potent hypoxia inducible factor-1 α (HIF-1 α) inhibitors. *Eur J Med Chem.* 2015;104:157-164.
31. Henry GE, Jacobs H. A short synthesis of 5-methoxy-2,2-dimethyl-2H-1-benzopyran-6-propanoic acid methyl ester. *Tetrahedron.* 2001;57:5335-5338
32. Roberts PJ, Der CJ. Targeting the Raf-MEK-ERK mitogen-activated protein kinase cascade for the treatment of cancer. *Oncogene.* 2007;26:3291-3310.
33. Sybyl-X. Version 2.1. St. Louis, MO: SYBYL molecular modeling software; 2013.

Investigation of B,C-Ring Truncated Deguelin Derivatives as Heat Shock Protein 90 (HSP90) Inhibitors for Use as Anti-Breast Cancer Agents

Ho Shin Kim, Van-Hai Hoang, Mannkyu Hong, Kyung Chul Kim, Jihyae Ann, Cong-Truong Nguyen, Ji Hae Seo, Hoon Choi, Jun Yong Kim, Kyu-Won Kim, Woong Sub Byun, Sangkook Lee, Seungbeom Lee, Young-Ger Suh, Jie Chen, Hyun-Ju Park, Tae-Min Cho, Ji Young Kim, Jae Hong Seo* Jeewoo Lee*



ACCEPTED MANUSCRIPT